# UNIVERSITÀ DEGLI STUDI DI CAGLIARI

**DIPARTIMENTO DI SCIENZE BIOMEDICHE**


## DOTTORATO DI RICERCA IN SCIENZE MORFOLOGICHE E FUNZIONALI

**CICLO XXVII**

Coordinatore: Prof.ssa Valeria Sogos

Settore Scientifico Disciplinare: BIO/16

# DIABETES-RELATED ULTRASTRUCTURAL AND IMMUNOHISTOCHEMICAL CHANGES IN HUMAN SALIVARY GLAND PARENCHYMA AND A STUDY ON A NATIVE SCAFFOLD OBTAINED FROM SALIVARY GLAND STROMA


Tutor/Relatore
**Prof.ssa Margherita Cossu**

Tesi della
**Dott.ssa Maria Alberta Lilliu**


Esame finale anno accademico 2013 – 2014

Maria Alberta Lillliu gratefully acknowledges Sardinia Regional Government for the financial support of her PhD scholarship (P.O.R. Sardegna F.S.E. Operational Programme of the Autonomous Region of Sardinia, European Social Fund 2007-2013 - Axis IV Human Resources, Objective l.3, Line of Activity l.3.1.)".

This work has been partially supported by the "Fondazione Banco di Sardegna".

## ABSTRACT

Systemic pathologies such as diabetes and Sjögren's syndrome, medications, and radiation therapy often affect salivary gland morphology and functionality, giving rise to changes in quantity and composition of saliva and to numerous oral complications that severely compromise the patient's life quality.

The aim of this thesis, articulated into two sections, was to evaluate:

1) if salivary gland morphology and functionality are affected by type 2 diabetes mellitus even when there are not evident signs of oral injuries;
2) the possibility to use a native scaffold derived from human salivary glands as a substrate in which salivary cells can be host to restore damaged salivary glands.

The first part of the investigations was carried out with surgical samples of salivary glands obtained from subjects, half diabetics and half non-diabetics, all without evident oral diseases. The samples were processed for light and electron microscopy and random images were subjected to morphometrical evaluation. The calculations revealed diabetes-related alterations such as acinar swelling and remarkable changes in serous cells, where secretory granules appeared enlarged but reduced in their total number. On the other hand, an increased number of granules anchored to the apical membrane was found, as well as an altered number of apical vesicles and microvilli (both involved in the mechanisms of membrane recycle). Taken together these findings suggest the occurrence of difficulties in the last step of exocytosis, and demonstrate that the structures involved in the secretory process are altered by diabetes *per se*. Other samples were analyzed by means of immunogold staining method to reveal the ultrastructural localization of melatonin and its receptors MT1 and MT2, until now never reported. Both melatonin and receptors were reactive in the secretory granules, in cytoplasmic vesicles and on cell surfaces, suggesting that their interaction could allow melatonin storage within specific cell compartments. Melatonin staining when performed on diabetic major salivary glands highlighted changes in the labeling intensity related with the diabetic condition.

The second part is focused on the characterization of a native salivary gland scaffold in view of its use in gland reconstruction. As well as diabetes, radiation therapy, Sjögren's syndrome, and several medications also give rise to salivary gland degeneration and xerostomia, but the therapies commonly used are not satisfactory so far. An emerging alternative approach to ameliorate the life quality of xerostomic patients is the regeneration of salivary parenchyma. A "Native Human Submandibular Gland Scaffold" (nHSMGS) was isolated from healthy submandibular glands, and was analyzed by light and electron microscopy and by histochemistry. Morphological examinations showed a fiber arrangement similar to that of the intact glands, while histochemistry revealed the presence of collagen type I, III, and IV. Then, a human salivary gland cell line and human fibroblasts were seeded and cultured on the scaffold in order to verify its reliability as autologous substrate for cells expansion. Results showed that a high cell percentage was proliferating after 4 days of culture, and that most cells were still alive after 8 days. All these data encourage the use of the nHSMGS as autologous scaffold in which expand salivary cells for the restoring of damaged salivary glands.

**Keywords**: Salivary glands, type 2 diabetes, melatonin, morphometry, histochemistry, native scaffold, tissue engineering.

**Corresponding author**: Maria Alberta Lilliu, Department of Biomedical Sciences, Section of Cytomorphology, University of Cagliari, 09042 Monserrato, Italy. E-mail: malilliu@unica.it

# TABLE OF CONTENTS

# INTRODUCTION

## *Saliva and Salivary Glands*

Saliva exerts several functions in the upper tract of the alimentary canal, classified as digestive and protective, resumed in Fig. 1. Digestive functions include food moistening needed to form bolus, to chew, and to swallow, enzymatic food degradation, and dissolution of tastants in order to interact with the taste buds. Protective functions include washing and lubrication of the oro-pharyngeal wall, remineralization of the tooth enamel, maintenance of the salivary pH, host defense against pathogens, and wound healing stimulation. Moreover, saliva has also additional functions, that are related with social interactions such as speech and kissing (Kaplan and Baum, 1993; Ekström and Khosravani, 2011).

Saliva is a hypotonic fluid composed by water (99%) and dissolved organic and inorganic molecules (1%). Among inorganic components, calcium and phosphate play important roles in the maintenance of tooth integrity, while bicarbonate allows buffering. The chief organic compounds are mucins with lubricating and protective properties and a large assortment of functionally different proteins as enzymes, antibodies, hormones, growth factors. Moreover, saliva contains numerous other substances, such as drugs and hormones, which directly come from blood so that their concentration in saliva reflects that in serum. Therefore, saliva is recognized as a mirror of the body's health and its use as diagnostic fluid offers many advantages over serum such as its cost-effectiveness and non-invasiveness. Saliva testing is now adopted not only to monitor drugs as alcohol and cocaine but also to diagnose diseases as allergies, cancer, HIV (Lawrence, 2002; Kaufman and Lamster, 2002; Pink *et al*, 2009; Deepa and Thirrunavukkarasu, 2010).

Saliva is secreted by a family of exocrine glands known as major and minor salivary glands. Major salivary glands are three pairs of glands called parotid, submandibular and sublingual that are located externally to the oral spaces and connected with the mouth by their excretory ducts (Fig. 2). Parotid gland embraces the mandible ramus and its main duct (Stensen's duct) opens opposite to the second upper molar. Submandibular gland is located under the

floor of the mouth near the mandible body and its main duct (Warton's duct) opens near to the lingual frenulum, while sublingual gland is on the mouth muscular floor and its numerous ducts open under the tongue. Minor salivary glands are hundreds of small glands which occupy the mucosal layer of the mouth, and their name is based on their location (lingual, buccal, labial, palatine). The amount of saliva secreted is 1-2 L /24h, 60% coming from submandibular glands, 30% from parotid glands, 5% from sublingual glands and the remaining 5% from the minor salivary glands (Dawes and Wood, 1973). Saliva can be considered as gland-specific and whole saliva, since the salivary fraction produced by each gland is similar but not identical to that from the others. Gland-specific saliva can be used to diagnose pathologies specific for one gland, whereas whole saliva is most frequently used to diagnose systemic diseases (Kaufman and Lamster, 2002).

Histologically, major salivary glands have a common general architecture (Riva *et al*, 1990). They are surrounded by a connective capsule that gives rise to septa, which contain vessels and nerves and divide the parenchyma into lobes and lobules. The glandular parenchyma consists in a secretory portion, represented by acini or tubuli, and a branched system of ducts that connect the secretory portion with the oral cavity (Fig. 3).

Secretory endpieces are classically distinguished into serous or mucous, based on their different staining with hematoxylin-eosin mixture. Serous cells have a basophilic cytoplasm, due to the RER abundance indicating their engagement in protein synthesis; mucous cells have a very clear cytoplasm, filled with unstained mucins (Tandler, 1978). Only serous secretory units are present in parotid, prevailingly serous in submandibular gland, prevailingly mucous in sublingual and in most of the minor salivary glands. Proteins secreted by serous cells are glycosylated proteins such as mucins, agglutinins, secretory IgA, amylase, glycosylated prolin-rich proteins (PRPs), and phosphorylated proteins such as acidic PRP, statherin, histatins. The most abundant are PRPs, multifunctional proteins that play important roles in the maintenance of the enamel pellicle, in lubrication, and in host defense, and amylase that starts the starch digestion in the mouth. The secretory products of mucous cells chiefly consist in mucins, highly glycosylated proteins represented by MG1 and MG2.

Both serous and mucous endpieces are surrounded by the long processes of myoepithelial cells, which aid secretion by squeezing acinar cells. Secretory endpieces are in continuity with the first and smallest segments of the ductal system, the intercalated ducts, formed by poorly specialized cells generally considered as reservoir or stem cells (Redman, 1987; Cutler, 1989). They join to form striated ducts, lined by mitochondrion-rich cells specialized in ion absorption; subsequent excretory interlobular ducts of progressively larger caliber join to form the main duct.

## *Ultrastructure of serous cells*

In spite of minor differences, serous cells of all major salivary glands share the basic structural features, so that an unique description applies to parotid and submandibular glands acinar cells. Serous cells are the site where the synthesis and secretion of the majority of the salivary proteins take place and also were the fluid is generated. Their secretion, called primary saliva, is an isotonic aqueous fluid which is transformed into the hypotonic final saliva during the passage along the striated ducts that actively absorb most $Na^+$ and $Cl^-$ ions of primary saliva and secrete small amounts of $K^+$ and $HCO_3^-$ (Baum, 1993).

At the ultrastructural level, the arrangement of the cell organelles is highly polarized: the most typical features are many basally packed rough endoplasmic reticulum (RER) cisternae, a prominent Golgi complex, and a variable number of secretory granules. Many mitochondria are located among the RER element in order to sustain the energetic cost of protein synthesis. According to the classic view (Palade, 1975) newly synthesized proteins are transported from RER to the Golgi complex where they undergo post-translational changes as glycosylation or removal of peptides or sugars. Then proteins are stored inside the secretory granules and finally released in response to stimulation into the acinar lumen. Even if the steps in the formation of secretory granules remain unclear, it seems that secretory proteins are packaged into immature secretory granules probably due to an interaction between secretory proteins, produced in the trans- Golgi network (TGN), and receptors in the TGN membranes (Tooze, 1998). Granules undergo maturation by concentrating and transforming their content, and are gradually directed

towards the luminal cell surface. Then, in response to specific signals, they undergo exocytosis, an energy-dependent process characterized by several steps (anchoring, docking, priming, triggering and fusing), culminating in the release of the granule content into the lumen. A crucial event in this process is the calcium dependent granule docking, consisting in the granule anchoring to the cell surface. In this phase the granule membrane and plasmalemma are ready to fuse as soon as the signal arrives. The extracellular signals that trigger exocytosis are usually chemical messengers, that often generate a transient increase in the cytosolic $Ca^{2+}$ concentration (Martin, 1997; Südhof, 2004). Once exocytosis is finished, the membrane arrangement is restored through the balance of the outward and inward membrane flows, provided by the formation of endocytotic vesicles.

## *Regulation of salivary secretion*

Salivary secretion depends on many regulatory systems which adapt it to functional requirements. The chiefly responsible for functional adaptive changes are the parasympathetic and sympathetic nervous systems, which cooperate in enabling salivary glands to vary the composition and amount of saliva according to the necessities. The primary parasympathetic centers are the superior salivatory nucleus in the pons and the inferior salivatory nucleus in the medulla oblongata, related with the facial nerve/submandibular ganglion and with the glossopharyngeal nerve/otic ganglion respectively. The sympathetic salivary center is located in the upper thoracic segments of the spinal cord. Postganglionic nerve terminals reach acini, ducts, and vessels, where the transmitters noradrenalin (sympathetic) and acetylcholine (parasympathetic) find a variety of receptors, particularly abundant in acinar cells. When noradrenalin stimulates $\beta_1$ receptors, the cyclic adenosine monophosphate (cAMP) system realizes a rapid increase of granule exocytose and consequent release of protein-rich saliva, while acting on $\alpha_1$ receptors, it rovokes a watery secretion. On the other hand, acetylcholine through muscarinic receptors $M_1$ and $M_3$ elicits $Ca^{2+}$ mobilization from intracellular stores and consequent release of a fluid saliva rich in water and electrolytes but with low amounts of proteins.

The greatest production of saliva occurs in a reflex way during eating in order to facilitate lubrication and initiate food digestion, but an ongoing modest salivation is also needed in order to ensure mouth health during the pauses. Acinar cells secrete even without stimulation through the so called constitutive secretion: small vesicles originated from the *trans*-Golgi network carry small amounts of proteins and open into the luminal or interstitial spaces. Other vesicles originate from immature secretory granules: some of them open into the lumen without stimulation (constitutive-like secretion), others in response to low level cholinergic and adrenergic stimulation (minor regulated secretion). Most literature data now agree that these three modalities are responsible for the resting saliva. During meals, high level stimulation causes the massive emptying of the large mature secretory granules (major regulated secretion), which begins when the granule membrane fuse with the apical plasmalemma (Castle and Castle, 1996; Castle and Castle, 1998; Huang *et al*, 2001).

## *Salivary Hypofunction*

Salivary gland malfunction results in inadequate secretion of saliva in terms of quantity and composition. Salivary hypofunction provides insufficient mouth lubrication and consequent difficulties in eating, swallowing, and speaking, and also poor protection against pathogens (Dodds *et al*, 2005). This condition, when greatly worsened, is called xerostomia, characterized by strong damages in the structures of the salivary gland parenchyma and has been demonstrate that this "dry mouth" sensation do not appear until a reduction of the 50% in salivary functions (Dawes, 1987). Xerostomia is often associated with systemic diseases such as Sjögren's syndrome, rheumatoid arthritis, diabetes mellitus, Parkinsonism, and hypertension (Fox, 2008). These diseases have in common basic metabolic alterations, such as an imbalance between the factors producing reactive oxygen radicals (ROS) and those involved in the protection against them (oxidative stress). Consequently the presence of inefficient macromolecules such as proteins, lipids, and nucleic acids compromises all the cell activities (Styskal *et al*, 2012).

## OUTLINE OF THE THESIS

Epidemiological studies have found an high correlation between diabetes mellitus and disorders of the oral tissues, among which one of the most aching is xerostomia, characterized by the progressive degeneration of salivary gland parenchyma (sialosis) largely documented. However, still is debated if salivary glands are affected by diabetes *per se*.

The first section of this thesis focuses on the secretory activity of human major salivary glands in subjects with type 2 diabetes mellitus (T2DM) with apparently normal salivation. The ultrastructural approach has been chosen to explore intracellular compartments where the secretory products travel before exocytosis in order to identify which step in the secretory process is affected by the diabetic status. Morphological and functional changes have been investigated by means of morphometrical and immunohistochemical analysis. These experiments were carried out in the Laboratory of Electron Microscopy at the University of Cagliari, place of my PhD.

As well as diabetes, many other causes have been identified for xerostomia, such as Sjögren's syndrome, radiation of the head and neck, and several medications so that this condition appears rather diffused. Since the treatments for xerostomic patients are not satisfactory so far, researchers are evaluating the possibility to regenerate damaged salivary glands through tissue engineering.

The second section of this thesis is focused on a tissue engineering project which I worked on during my experience as a Graduate Research Trainee at the Laboratory of Craniofacial Tissue Engineering and Stem Cells at McGill University. The goal of this project was to test if a native Human salivary gland scaffold may be able to provide a good autologous substrate in which salivary cells can be expanded. Light and electron microscopy has been utilized to evaluate the morphology of this scaffold and the presence of extracellular matrix components. The interactions between scaffold and cells have been also evaluated through viability and proliferation assays.

# SECTION 1: TYPE 2 DIABETES MELLITUS AND SALIVARY GLANDS

## *Type 2 diabetes mellitus and oral health*

Type 2 diabetes mellitus is a chronic disease that occurs when the body cannot effectively use the insulin it produces, since there is a failure of the insulin signaling mechanism in the target cells of the body. Defined as a new epidemic worldwide, type 2 diabetes is expected to increase severely by the coming 15 years (Leite *et al*, 2013). In 2014, World Health Organization (WHO) estimates that 9% of adult population (18+ years old) around the world is affected by diabetes and the 90% of this is represented by T2DM. Hyperglycemia, which characterizes the diabetic condition, is considered as a key factor for the manifestation of side disorders in several organs. Nephropathy, retinopathy, neuropathy, delayed wound healing and cardiovascular pathologies such as coronary arterial disease and stroke, are the five common complications of diabetes (Leite *et al*, 2013). Epidemiological studies have described an high correlation between diabetes mellitus and oral cavity disorders, identifying thus the periodontal disease as the "sixth complication" of diabetes (Loe H, 1993).

Periodontitis, candidiasis, gingivitis, dental caries, tooth loss, taste impairment, and xerostomia, frequently afflict diabetic patients and severely worsen their quality of life. They are often associated with inadequate salivation and with degenerative alteration of salivary glands defined as sialadenosis (Donath and Seifert, 1975; Ben-Aryeh *et al*, 1993; Dodds *et al*, 2000; Carda *et al*, 2006). In diabetic animal models, the morphological alterations of salivary glands have been extensively demonstrated (Hand and Weiss, 1984; Anderson *et al*, 1990) and some studies demonstrated that after insulin treatment, diabetes alterations were only reduced but not completely abolished (Chan *et al*, 1993; Caldeira *et al*, 2005). However, given the diversities between the salivary glands of the two species and also the numerous substances used to induce diabetes, data regarding animals are only partially comparable with those of humans.

In diabetic patients without periodontal diseases or sialosis salivary function is generally considered as a normal and the salivary gland morphology has not been investigated accurately since assumed as normal. Only a few studies on

whole saliva have reported alterations of salivary flow and composition imputable to diabetes *per se* (Dodds and Dodds, 1997; Dodds *et al*, 2000; Mata *et al*, 2004; Barnes *et al*, 2014). Recent studies of my laboratory group showed a reduced statherin expression in apparently normal salivary glands of diabetic patients (Isola *et al*, 2011a; 2011b; 2012). Since functional variations usually are accompanied by morphological changes, I decided to analyze by morphometrical analysis, submandibular and parotid glands from diabetic patients in order to detect ultrastructural alterations so minute as not to be detectable at the mere observation. Particular attention has been directed to the serous cells and specifically to those cellular structures directly involved in the protein secretion. Dimension of serous acini, and dimension and number of secretory granules, have been analyzed by light and electron microscopy. Moreover, submandibular gland data were compared with parotid once. In fact, it appears reasonable that the two glands may be affected differently by diabetes, due to their numerous peculiarities both in morphology and in physiology.

## *Melatonin and salivary glands*

Melatonin is an idoleamine principally released from the pineal gland and synthesized starting from the amino acid tryptophan via 5-hydroxytryptamine. Extrapineal sources of this hormone have been identified in many tissues such as brain, retina, pancreas, liver, gastrointestinal tract, that contain also the enzymes involved in its synthesis (Kvetnoy, 1999). Being a lipophilic substance, melatonin can pass freely the cell membranes so that it is believed to reach by diffusion all peripheral tissues and biological fluids such as cerebrospinal fluid, saliva, amniotic fluid, synovial fluid, in which it can reach concentrations higher than in blood (Acuña-Castroviejo *et al*, 2014). However, this belief has been recently questioned (Hevia *et al*, 2008; 2015). Although its main function is regulate night and day cycles, melatonin exerts also protective, anticancer, immunomodulatory, antioxidant and anti-inflammatory properties (Galano *et al*, 2011). Apart from receptor-independent free radical scavenging actions, the majority of melatonin functions are mediated by nearly ubiquitous specific melatonin receptors $Mel_{1A}$ (MT1) and $Mel_{1B}$ (MT2), members of the family of G

proteins-coupled receptors with seven transmembrane domains. Melatonin, acting on these receptors causes changes in calcium and potassium channels and also modulates several intracellular signals such as adenylate cyclase, guanylyl cyclase, phospholipase $A_2$ and C (Galano *et al*, 2011; Reiter, 2015). In addition, immunomodulatory and protective functions are mediated by a group of nuclear receptors named ROR/RZR family (retinoic acid-related orphan receptor/retinoid Z receptor) (Mauriz *et al*, 2013). MT1 and MT2 receptors are often colocalized, but their activation can exert divergent and/or opposite physiological effects (Dubocovich and Markowska, 2005). Both MT1 and MT2 receptors have been localized by immunoblotting in rat parotid glands (Aras and Ekström, 2008), while with regard to human salivary glands MT1 receptors were localized by light microscopy in parotid and submandibular glands (Arias-Santiago *et al*, 2012; Aneiros-Fernandez *et al*, 2013). Light microscopy however, is not enough to understand the fine intracellular localization of this receptors. Using a post-embedding immunogold technique I thus decided to verify the expression of MT1 and MT2 receptors in human parotid glands to better understand in which intracellular compartments are localized and if they may be also involved in the traffic of melatonin.

Saliva contains only the free form of melatonin, while blood contains both the albumin bound (70%) and the free (30%) forms. It is generally accepted that salivary melatonin corresponds to the 30% of blood melatonin (free form) and that it comes directly from blood crossing passively the salivary gland cells (Cengiz *et al*, 2012; Reiter *et al*, 2015). However, it has been demonstrated that the concentration of melatonin in saliva does not always reflect that of blood (Laasko *et al*, 1990). Moreover, a local production has been recently suggested by the finding of the melatonin-synthesizing enzymes N-acetyltransferase and hydroxyindole-O-methyltransferase in rat and human salivary glands (Shimozuma *et al*, 2011).

Since until now, melatonin ultrastructural localization in human salivary glands has never been reported, I have performed an immunohistochemical investigation on parotid and submandibular glands in order to gain information about the intracellular route of the hormone. It appeared

predictable that, due its lipophilic nature, melatonin can be extracted during sample preparation, unless bound to other molecules and stored in cell compartments as proposed by Venegas *et al* (2012).

Like many other components of saliva, melatonin changes its concentration in certain conditions: altered levels of salivary melatonin are associated to diabetic status and oral diseases causing inadequate protection of the oral cavity (Cutando *et al*, 2003; Almughrabi *et al*, 2013; Abdolsamadi *et al*, 2014). This has been explained by Reiter *et al* (2015) as consequence of a general reduction of serum melatonin level (less melatonin in the blood, less melatonin in saliva), or of a quick consumption of melatonin for free radicals detoxification in the oral cavity. Moreover, in order to understand if the diabetes-related alterations of melatonin observed in fluids are remarkable also in the glandular parenchyma I decided to verify the expression of melatonin also in diabetic major salivary glands.

## *Aim of the section*

The hypothesis of this project is that the diabetes-related alterations occur in salivary gland parenchyma even in absence of evident oral pathologies. This section deals with the ultrastructural features and melatonin distribution in normal and diabetic salivary glands, with particular attention to the serous secreting cells. Objectives of this section were:

- To detect by morphometry diabetes-related changes in the salivary gland parenchyma
- To localize melatonin and its receptors at the ultrastructural level

# MATERIALS AND METHODS

## *Morphometrical analysis*

### *Patients*

Fragments of submandibular and parotid glands were obtained from a total of 40 patients (male, mean age 60) undergoing surgery for the excision of cancers from the oral region at the Otorhinolaryngology Clinic, University of Cagliari. Patients were not alcohol consumers, smokers, obese or affected by autoimmune diseases, and had no signs of oral diseases such as xerostomia, periodontitis, or taste dysfunctions. Half of the subjects were affected by diagnosed type 2 diabetes mellitus and the glycemic level was controlled either by diet or medicines. The sample cohort was divided for each gland into two groups: diabetics and non-diabetics. All the procedures were approved by the local Institutional Committee for human experimentation at the ASL 8 (Azienda Sanitaria Locale 8), Cagliari, and a written informed consent was obtained from all patients.

### *Sample preparation*

For light microscopy (LM) and transmission electron microscopy (TEM) the samples were cut in small pieces (around 2 $mm^3$) and fixed for 2 hours at room temperature with a mixture of paraformaldehyde (1%) and glutaraldehyde (1,25%) in 0.1 M sodium cacodylate buffer (pH 7.2). The pieces were then rinsed in cacodylate buffer plus 3,5% sucrose, fixed with $OsO_4$ (2%), dehydrated with acetones scale, embedded in Epon Resin (Glycide Ether 100; Merck, Darmstadt, Germany), and left in a 60° C oven for 48 hours. Randomly chosen tissue blocks from each patients were cut under an ultramicrotome using a diamond knife, into semi-thin (1 μm) and ultra-thin (90-100 nm) sections. Semi-thin sections were stained with toluidine blue and examined with a Leica DMR microscope equipped with a CCD Camera (Leica DC 300). The ultra-thin sections were collected on copper grids, stained with uranyl acetate and bismuth subnitrate,

then examined and photographed with a JEOL 100S transmission electron microscope.

For high resolution scanning electron microscope (HRSEM) the samples were cut into small pieces (around 1 $mm^3$) and fixed for 15 minutes with a mixture of paraformaldehyde (0,2%) and glutaraldehyde (0,25%) in 0.1 M sodium cacodylate buffer (pH 7.2). After post-fixation with a mixture of $OsO_4$ and $K_3[Fe(CN)_6]$ the samples were cut in thin slices (150 μm), post-fixed for one more time and then exposed to our variant of the osmium maceration method in order to visualize the cytoplasmic side of plasma membrane (Riva *et al*, 2007). Samples were dehydrated, exsiccated using a critical point dryer, mounted in stubs, coated with 20 nm of platinum and then examined with a Hitachi S4000 FEG HRSEM operating at 15–20 kV.

## *Immunohistochemistry by immunogold labeling*

### *Patients*

For melatonin labeling, fragments from a total of 20 submandibular and parotid glands were obtained from consenting male patient (mean age 60) undergoing surgery for the excision of cancers from the oral region at the Otorhinolaryngology Clinic, University of Cagliari. Samples were collected at about 11:00 AM. Half subjects were affected by type 2 diabetes mellitus, selected as those described for the morphometrical analysis.

For the detection of melatonin receptors fragments of parotid glands were obtained from eight patients, five males and three females, aged 40–65 years, undergoing surgery for the removal of tumors of the neck region at the Otorhinolaryngology Clinic, University of Cagliari. Samples were collected at about 11:00 AM. Patients were not habitual smokers, alcohol consumers or obese, and were not affected by autoimmune diseases or subjected to chemotherapy or radiotherapy before surgery.

*Experimental procedures*

Fragments were cut into small pieces and fixed for 2 hours with a solution of paraformaldehyde (3%) and glutaraldehyde (0,1%) in 0.1 M sodium cacodylate buffer (pH 7.2). After rinsing in sodium cacodilate buffer + 3,5% of sucrose samples were dehydrated with a scale of acetones and embedded in Epon resin. Randomly chosen blocks of each sample were cut under an ultramicrotome into ultrathin sections (80-90 nm) which were collected on nickel grids.

Grids were then hydrated with phosphate buffered saline (PBS) and then incubated with a blocking solution of PBS + 1% bovine serum albumin (BSA) + 5% normal goat serum (NGS) in order to block non-specific binding. The grids were then incubated over night at 4° C with the primary antibodies: a rabbit polyclonal antibody specific for either MT1 or MT2 (abcam, Cambridge Science Park, Cambridge, UK), diluted 1 : 50 in 1% BSA-PBS + 5% NGS and a rabbit polyclonal anti-melatonin antibody (dilution 1: 20, Thermo Fisher Scientific Inc., USA). Controls were incubated with a non immune rabbit serum or omitting the primary antibody. The following day the grids were incubated in the second blocking solution (1% BSA-PBS) for 30 minutes. A goat anti-rabbit IgG secondary antibody conjugated with 15 nm gold particles (GE Healthcare, UK) diluted 1: 30 with 1% BSA-PBS was then applied for 1h at room temperature. After washing with PBS and distilled water grids were stained with uranyl acetate and bismuth subnitrate, and observed with a transmission electron microscope (JEOL 100S at 80Kv). Pictures of secretory cells were taken from at least two grids for each patient, and then examined in order to evaluate the localization and the gold particle density.

## *Image analysis*

The micrographs were analyzed using the imaging software Image Pro Plus (Media Cybernetics, Inc.) both for the morphometrical and for the immunohistochemical studies.

In randomly chosen LM images, a number of at least 20 serous acini for sample were evaluated in each gland type in order to calculate the area occupied by serous acini and the number of intracellular lipid droplets/ $\mu m^2$.

In randomly chosen TEM micrographs a mean of 50 secretory granules from each patient were evaluated for each gland type in order to calculate their total area and their number/ 100 $\mu m^2$. The thickness of the basal lamina also was measured.

In randomly chosen HRSEM images (15 pictures/sample) were analyzed in order to evaluate the inner side of the apical membrane and its specializations such as microvilli, microbuds and protrusions.

To evaluate the melatonin labeling, 5 TEM micrographs of acinar cells for each sample were randomly chosen and analyzed. Since melatonin labeling was chiefly stained in secretory granules the morphometric analysis were focused only on these organelles. A total of 600 granules (half from diabetics and half from non-diabetics) were analized both for submandibular and parotid glands in order to evaluate the labeling density, expressed as number of particles/$\mu m^2$.

## *Statistical analysis*

All the values obtained were expressed as a mean ± standard error mean (SEM) and analyzed for the statistic using the unpaired Student's t-test with Welch's correction and the Mann-Whitney test. P values < 0,05 represent statistically significant differences between diabetic (D) and non-diabetic (ND) groups.

# RESULTS

## *Morphometrical analysis*

### *Light microscopy*

In LM images (Fig. 4) of submandibular (a, b) and parotid (c, d) glands, no appreciable differences between diabetic and non-diabetic samples are detectable at the mere observation. Both glands show serous acini with the typical pyramidal cells arranged around the small lumen, where nuclei secretory granules are well recognizable. Morphometrical evaluation (Fig. 5) highlights a significant enlargement of serous acini in diabetic submandibular glands (mean area 471 $\mu m^2$) with respect to non-diabetic (398 $\mu m^2$), while statistically significant differences do not result in parotid samples. Lipid droplets density remains unchanged in all the samples.

### *Transmission electron microscopy*

In TEM images (Fig. 6) of submandibular (a, b) and parotid (c, d) glands, no appreciable differences between ultrastructural features of diabetic and non-diabetic samples are detectable at the mere observation. Morphometrical evaluation (Fig. 7) shows a significant increase of secretory granules area in diabetic submandibular glands (0,430 $\mu m^2$) with respect to non-diabetics (0,340 $\mu m^2$), while no significant differences results for parotid glands. The number of granules tends to be reduced in diabetic submandibular glands, while remains unchanged in parotid glands. The thickness of the basal lamina shows a tendency to increase in diabetics.

## *High resolution scanning electron microscopy*

In HRSEM images (Fig. 8), unlike from LM and TEM, differences between diabetic and non-diabetic samples are appreciable from the mere observation and confirmed by morphometrical evaluation. Significant changes (Fig. 9) result

in the number of luminal membrane specializations examined by the plasmalemmal cytoplasmic side. Diabetic samples of both glands show a reduction in number of the holes corresponding to the base of microvilli (arrows), and an increased number of roundish structures attached to the membrane, the larger (protrusions) corresponding to the docked secretory granules (asterisks), the smaller (microbuds) corresponding to apical vesicles (arrowheads).

| | | Submandibular | | | Parotid | | |
|---|---|---|---|---|---|---|---|
| **Parameter** | **Microscope** | **ND** | **D** | | **ND** | **D** | |
| Area of serous acini ($\mu m^2$) | LM | 397,8 ± 21,73 | 470,9 ± 29,97 | * | 388,3 ± 21,47 | 369,9 ± 30,30 | |
| Number of lipid droplets / $\mu m^2$ | LM | 0,037 ± 0,017 | 0,049 ± 0,009 | | 0,048 ± 0,008 | 0,048 ± 0,006 | |
| Area of secretory granules ($\mu m^2$) | TEM | 0,343 ± 0,011 | 0,429 ± 0,015 | *** | 0,573 ± 0,013 | 0,574 ± 0,014 | |
| Number of secretory granules / 100 $\mu m^2$ | TEM | 83 ± 4,9 | 61 ± 7,4 | | 58,5 ± 8 | 58,7 ± 9 | |
| Thickness of basal lamina (μm) | TEM | 0,127 ± 0,021 | 0,164 ± 0,006 | | 0,073 ± 0,015 | 0,118 ± 0,019 | |
| Number of microvilli/ $\mu m^2$ | HRSEM | 29,67 ± 1,499 | 19,6 ± 1,519 | *** | 27,05 ± 1,716 | 20,83 ± 1,368 | ** |
| Number of microbuds/ $\mu m^2$ | HRSEM | 2,632 ± 0,273 | 3,594 ± 0,290 | * | 4,402 ± 0,513 | 7,785 ± 0,937 | ** |
| Number of protrusions/ $\mu m^2$ | HRSEM | 0,152 ± 0,036 | 0,535 ± 0,067 | *** | 0,191 ± 0,070 | 0,701 ± 0,104 | *** |

***P < 0,05 ** P < 0,01 *** P < 0,001**

Table. 1. Mean values (± SEM) of the variables analyzed in diabetic and non-diabetic submandibular and parotid glands.

## *Immunohistochemistry*

### *Melatonin labeling*

Immunogold experiments clearly show melatonin reactivity in both parotid and submandibular glands. In serous acinar cells of all the glands, the preferential sites of melatonin labeling are the secretory granules, and, when the bipartite structure is evident, the staining is restricted to the pale peripheral portion. Moreover, reactive small vesicles often appear around and among the granules, and near to the basolateral surfaces. A moderate staining is also seen on the cell membrane, especially in its basolateral portion. The mere observation

highlights a stronger reactivity in parotid with respect to submandibular glands (Fig. 10). Morphometrical evaluation focused on the serous granules, confirms this impression in that in parotid the 89% of total granules expresses melatonin reactivity, while in submandibular only the 42%.

In diabetic samples (Fig. 11) the pattern of melatonin labeling results unchanged with respect to non-diabetic ones. The quantitative evaluation shows a diabetes-related reduction in the percentage of labeled granules (8% for parotid and 7% for subamndibular). The labeling density in non diabetic samples is 28,12/$\mu m^2$ in the parotid, and 12,64/$\mu m^2$ in the submandibular, while in diabetics is 32,08/$\mu m^2$ in parotid, and 13,60/$\mu m^2$ in submandibular glands. Statistical analysis for the labeling density shows a significant increase of 14% ($P < 0,05$) in parotid glands, while a tendency to increase of 7,5% in submandibular glands (Fig. 12).

In both diabetic and non-diabetic samples, gold particles only occasionally are seen in intercalated duct cells, while striated duct cells show a moderate reactivity within small vesicles throughout the cytoplasma and near the basolateral surfaces (Fig. 13). Controls were always negative (Fig. 14).

***Melatonin receptors MT1 and MT2 expression in Parotid glands***

Gold particles labeling MT1 receptor (Fig. 15) are mainly localized in acinar cells within secretory granules, small vesicles scattered throughout the cytoplasm, and on basolateral membranes. In intercalated duct cells, reactivity is observed in vesicles close to the cell surfaces, but not in secretory granules. In striated duct cells a modest labeling results in nearly ubiquitous vesicles and in the basal folds of the plasmalemma. Nuclei and mitochondria only rarely are labeled in acinar and ductal cells (Fig. 16).

Immunoreactvity for MT2 (Fig. 17) is similar to that of MT1, even if the number of gold particles appears much lower. Moreover, MT2 reactivity in cells membranes is only occasional.

Control samples did not exhibit positivity for both antibodies (Fig. 18).

# DISCUSSION

The results of this investigation demonstrate that acinar cells of human salivary glands change their features in diabetic status even in absence of sialosis, substantiating the concept that diabetes *per se* affects their functions.

The most interesting results of the morphometrical analysis concern secretory granules of serous cells. Calculated with TEM images, the granule area increases while the granule number tends to decrease, suggesting either a reduced secretory activity or a major tendency of granules to fuse with each other before exocytosis. On the other hand, data obtained with the HRSEM analysis reveal an increased number of apically docked granules, whose augmentation has been interpreted by Loy *et al* (2012; 2014) as indicative of intensified secretion. In an attempt to reconcile these data, it can be assumed that secretory granules at the end of their intracellular route take longer to achieve exocytosis maybe due to some impediment to release their content. Thus, they would remain longer attached to the plasmalemma waiting to conclude the exocytosis; during this waiting time they would undergo abnormal swelling and coalescence. This would mean that diabetes makes something abnormal happen when granules are stored at the cell apex during the last secretory phases. This hypothesis finds confirmation in the data obtained counting microvilli and vesicles, whose altered density could further testify defects in exocytosis and subsequent membrane recycle in diabetic glands. A critical factor in determining these defects could be identified in intracellular concentration of $Ca^{2+}$, which represents the second messenger in many signaling pathways and regulates the functions of ion and water channels involved in electrolyte balance and fluid secretion. Besides, salivary gland dysfunction in diabetes and Sjögren's Syndrome is related with disturbances in calcium signaling and ion channel activities with consequent damages on several cell functions including secretion (Fedirko *et al*, 2006; Ambudkar, 2014; Zarain-Herzberg *et al*, 2014). Thus, impaired glucose metabolism and calcium imbalance, with consequent changes in cell osmolarity, presumably result in the swelling of acini as well as of secretory granules. Besides, like other diabetes-related metabolic defects, the impairment of

calcium balance can be ascribed to hyperglycemia and high intracellular glucose concentration, that cause accumulation of glycated products and ROS giving rise to oxidative stress. Secretory proteins also are affected, since changes in secretory products resulted from biochemical assays of diabetic saliva, and from immunohistochemical analysis of diabetic salivary glands (Dodds and Dodds 1997; Dodds *et al*, 2000; Mata *et al*, 2004; Carda *et al*, 2006). For example, the group of M. Isola has recently reported a significantly reduced expression of statherin, a protein involved in the maintenance of calcium homeostasis and tooth protection, by means of quantitative evaluation of immunoreactivity in salivary acinar granules (Isola *et al*, 2011a; 2011b; 2012). This thesis shows another change in the granule content, highlighted by the experiments on melatonin histochemistry. The results show highly significant differences in labeling density, but their interpretation appears rather problematical: the stronger labeling in diabetic acinar granules, especially in parotid, apparently indicates an increased melatonin secretion, while the reduced number of labeled granules suggests the contrary. Besides, literature on this topic, although scarce and contradictory, reports a reduction of melatonin in both saliva and serum of diabetics (Cutando *et al*, 2003; Abdolsamadi *et al*, 2014), explained with an impairment in the systemic production of melatonin (less melatonin in the blood, less melatonin in saliva) or with its augmented employment as radical scavenger (Reiter *et al*, 2015).

The histochemical experiments highlight a remarkable aspect of the intracellular route of melatonin and its receptors in serous cells. Melatonin localization within secretory granules indicates that it is segregated and stored together with most secretory products, waiting exocytosis. This could mean that the hormone reaches saliva not only through passive diffusion from blood as postulated by several authors (Cengiz *et al*, 2012; Acuna-Castroviejo *et al*, 2014; Reiter *et al*, 2015), but also through the regulated secretion by acinar cells. In addition, the labeled vesicles scattered among the granules could be interpreted as signs of constitutive-like or minor regulated secretion, through which melatonin could become available in resting saliva. However, the mechanism by which this small lipophilic molecule is accumulated in granules and vesicles still is obscure. According to recent studies (Hevia *et al*, 2008; 2015; Venegas *et al*, 2012) this mechanism should require the involvement of carries

which capture melatonin, prevent its diffusion through the membranes, and allow its concentration in storage compartments. Although excluded by Venegas *et al* (2012) based on pharmacological tests, MT1 and MT2 receptors might be plausible candidates for this role: like melatonin, they also react in the cell surfaces and in cytoplasmic vesicles, suggesting their involvement not only in mediating the hormone effects but also in the melatonin transport into storage sites, including secretory granules. This hypothesis is supported not only by the finding of both melatonin and receptors, chiefly MT1, within the granules but also by the stronger melatonin labeling at the granule periphery, indicative of its connection with the limiting membrane. Striated duct cells also appear reactive for both melatonin and receptors in surfaces and vesicles, though less than serous cells, so that a similar mechanism of melatonin transport could be proposed. On the other hand, striated duct cells seem to be able to produce the hormone, since they express the enzymes that convert serotonin into melatonin (Shimozuma *et al*, 2011). To date, only melatonin receptors MT1 have been confirmed in the membranes of ducts (Arias-Santiago *et al*, 2012; Aneiros-Fernandez *et al*, 2013), while no further evidence relating to melatonin production or secretion have been furnished.

The results of melatonin labeling clearly show an intense reactivity in parotid glands, and moderate in submandibular glands, confirming thus that these glands are both involved in the melatonin traffic (Reiter *et al*, 2015) and indicating that melatonin is unequally distributed in their parenchyma, being parotid glands the most involved in the melatonin trafficking from the bloodstream to the saliva.

Taken together, the morphometrical and immunohistochemical results show that parotid and submandibular glands are differently affected by diabetic condition, since some parameters appear largely modified in diabetic submandibular, less in parotid glands. This does not surprise, because even if it is generally thought that the two glands are equally sensible to diabetes, it is known that some pathologies affect more one gland rather than the other. In example, sialolithiasis affects more frequently submandibular than parotid gland (Huoh and Eisele, 2011), while neoplasies involve chiefly parotid (Nagler and Laufer, 1997); radiation damages involve mostly parotid (Jeong *et al*, 2013),

while xerostomia related to Sjögren's Syndrome is typically associated to submandibular dysfunctions (Güne *et al*, 2010). Moreover, anatomical features such as innervations and vascularization, histological and histochemical properties, embryonic origin, genetic, and metabolic aspects distinguish parotid from submandibular gland (Denny *et al*, 1997; Riva *et al*, 1990; Tandler and Phillips, 1993; Miletich, 2010).

## SECTION 2 : A MODEL OF NATIVE HUMAN SUBMANDIBULAR GLAND SCAFFOLD

### *Regeneration of salivary glands*

Xerostomia, as previously explained, consists in a sensation of dryness of the mouth derived from a reduced amount of saliva, that has as consequences inflammation, periodontal disease and augmented bacterial infections. There is a strong body of evidence that supports the relationship between salivary glands impairments and radiation therapy for head and neck cancers, where xerostomia represents one of the major consequences. Moreover, xerostomia is a common side effect of several medications, and is often associated to systemic pathologies such as diabetes mellitus and Sjögren's syndrome (Guggenheimer and Moore, 2003; Fox, 2008; Saleh *et al*, 2015). In this condition salivary glands show severe histological alterations such as necrotic parenchyma, fibrotic stroma, lymphocytic infiltrations and inflamed areas. Prescriptions for artificial saliva, moisturizers and medications which induced salivation from the residual tissue, even if not satisfactory, are the common strategies used to ameliorate the life of xerostomic patients (Chambers *et al*, 2004; Kagami et al, 2008). New promising treatments are under investigation, involving the use of stem cells to regenerate damaged salivary glands and to restore a normal salivation. Efforts of regenerative medicine in improving the tissue regenerative capacity are based on cell manipulation and on the use of growth factors and of adequate support for cell growth (Mattei *et al*, 2014; Zhao *et al*, 2013).

### *Scaffolds for tissue engineering*

An important challenge in building artificial tissues is to supply the cells with a suitable supporting structure, named scaffold, which reproduces the original extracellular environment.

In solid organs such as salivary glands, tissue organization and cell behavior strictly depend on the interactions between the cells and the surrounding

extracellular matrix (ECM). ECM is a complex of proteins such as laminin, collagen type I, III, IV, and fibronectin that are secreted by epithelial cells and fibroblasts. The ECM can be distinguished into two main regions: the basal lamina, a thin layer of laminin, fibronectin and collagen type IV, to which epithelial cells directly anchor, and the lamina fibroreticularis, composed by collagen type I and III secreted by fibroblasts, deeply connected with the stroma. ECM is not only a mechanical support for the cells, but is also necessary for many cell activities such as differentiation, migration and proliferation through its signaling properties.

In an attempt to optimize tissue replacement, many cell types are utilized such as stem cells or immortalized cell lines, as well as various natural or synthetic scaffolds with different physicochemical characteristics. Cell activities are strongly influenced by the matrix used for their culture: three-dimensional (3-D) matrices appear more suitable than two-dimensional (2-D) for reproducing the natural microenvironment (Hakkinen *et al*, 2011; Campbell *et al*, 2014; Walters and Gentleman, 2015). Scaffolds mimic the ECM not only in supplying a support for the cells, but also in regulating cell activities. In regenerative medicine, the use of biological decellularized native scaffolds is becoming progressively more frequent, satisfying the necessity to obtain native scaffolds able to maintain as much as possible the natural architecture of the tissue matrix. Moreover, based on their capacity to supply ECM proteins needed to recreate the in-vivo environment, native scaffolds are considered as more appropriate than artificial supports which need to be coated with exogenous ECM proteins (Mattei *et al*, 2014; Zhao *et al*, 2013; Campbell *et al*, 2014).

## *Native human salivary gland scaffold and cells*

To repair damaged salivary glands, the expansion of primary salivary cells from healthy glands appears as the method of choice, but there are numerous difficulties in maintaining primary salivary cells in long-term culture (Jang *et al*, 2015). Thus, salivary cell lines are commonly used as a convenient model to study cell behavior in vitro. The "Human submandibular gland" cell line (HSG), an immortalized cell line derived from an irradiated and non malignant

human submandibular gland (Shirasuna *et al*, 1981), is frequently used by several authors as a model of salivary gland cells (Wang *et al*, 1999; Aframian *et al*, 2002; Nagy *et al*, 2007; Maria *et al*, 2011a). Numerous experiments have demonstrated their ability to expand more rapidly when compared to primary salivary cells, to express salivary glands markers (i.e. aquaporin-5, α-amylase, vimentin) and also to grow in several scaffold types (Aframian *et al*, 2000; Maria *et al*, 2011a).

It has been demonstrated that the same cell types change their behavior when cultured on surfaces with different properties (Aframian *et al*, 2002; Maria *et al*, 2011a, Yamada *et al*, 2012). Therefore, various materials are utilized to obtain scaffolds with different properties to test cell behavior. Many approaches to regenerate salivary glands are mainly concentrated on the use of 3-D gel substrates and flat polymeric surfaces (Soscia *et al*, 2013) such as poly-L-lactic acid (PLLA), polyglycolic acid (PGA), poly-lactic-co-glycolic acid (PLGA) and chitosan (Cantara *et al*, 2012; Aframian *et al*, 2000; Joraku *et al*, 2005; Chen *et al*, 2005).

In addition to artificial polymers, natural supports have been used to host salivary gland cells: Wang et al in 1999, for example, have demonstrated cell growth with a denuded rat trachea. Both synthetic and biological scaffolds often are coated with ECM proteins such as laminin, fibronectin and collagens in order to increase their efficiency (Wang *et al*, 1999; Aframian *et al*, 2000; Chen *et al*, 2005; Cantara *et al*, 2012).

Much efforts have focused on culturing salivary epithelial cells on scaffolds. It is worth remembering in addition to the salivary epithelial cells population (parenchyma), another major cell population is the fibroblasts (in the stroma). Interactions of epithelial cells with the mesenchyme are important during organ development. Working with the research group of Professor Simon D Tran, I wanted to simulate this condition in vitro by seeding a mixture of salivary epithelial cells with fibroblasts on the native human submandibular gland scaffold. The fibroblasts used in our experiments were from a primary cell culture of "Human Foreskin Fibroblasts" (HFF). These fibroblasts are widely used in cell biology experiments (Tran H *et al*, 2002; Hakkinen *et al*, 2011) and can be expanded rapidly.

The intent of this project was to isolate a "Native Human Submandibular Gland Scaffold" (nHSMGS) from healthy submandibular glands and verify its potential use as a substrate to expand salivary gland cells. One convenient advantage of nHSMGS is that tissue remnants that are usually discarded following salivary cells isolation are now kept and are to be used as (autologous) scaffolds for engineering of salivary glands. To verify if these nHSMGS have maintained properties of the original salivary tissue, we repopulated this scaffold with primary culture cells. However, given the difficulties derived by their use, I preferred the HSG, which can be more easily handled and can grow much quicker. A primary culture of HFF was also added to simulate the original tissue.

## *Aim of the section*

The hypothesis is that the "native human submandibular gland scaffold" (nHSMGS) provides a good support for salivary gland growth and possesses the properties to facilitate cell adhesion and proliferation. Objectives of this project were to demonstrate:

- Morphology of the native scaffold
- Presence of ECM proteins
- Cell proliferation
- Cell viability

# MATERIALS AND METHODS

## *Isolation of the nHSMGS*

Human submandibular gland biopsies (n=5) were obtained from the Departments of Otolaryngology, and Oral and Maxillofacial Surgery, McGill University, Montreal. The glands (all from men, mean age 58) were excised during surgery for the removal of neck and head cancers. All patients had received no radiotherapy or chemotherapy and all glands were histologically judged normal. Large pieces of the removed glands were processed to obtain the nHSMGS, while small pieces were destined to other experiments. Fragments of intact glands were used as controls.

In order to obtain the native scaffold, the pieces were washed with DMEM-Dulbecco's Modified Eagle Medium (Gibco, Life Technologies Inc., Gaithersburg, MD) + 5% of Gibco Antibiotic-Antimycotic (Life Technologies) and then processed according to the method for salivary gland cell isolation described by Tran *et al*, (2005) and Maria *et al*, (2011b). Briefly, the glands were mechanically minced and enzymatically/mechanically digested using DMEM-Dulbecco's Modified Eagle Medium + Hyaluronidase and Liberase (0,035mg/L) combined to a Gentle Macs Dissociator (Miltenyi Biotec). The nHSMGS consisted in the connective tissue, which remained after filtration through a 70 μm strainer. Scaffolds were immediately transferred in cell culture dishes and incubated at 37°C. Some of them were destined for electron microscopy and processed as described later, while other were destined for light microscopy experiments and treated as follows modifying the protocol showed by Campbell et al (2014). Scaffolds were embedded in Optimal cutting temperature (O.C.T.) and immediately placed at -80°C. The tissue was then sectioned under a cryostat (Leica CM 3050 S) in 12 μm sections captured in positively charged microslides (Fisherbrand Superfrost Plus Microscope Slides) and stored at -80°C.

## *Light Microscopy*

### *Collagen detection by Sirius red*

Picro-sirius red staining (2610-10-8, Alfa Aesar) was used in order to verify the presence of collagens in the nHSMGS. Cryo-sections of 12 μm were first stained with Weigert's hematoxylin (Fisher scientific) and then with picro-sirius red for 1h. After being washed with acidified water, the slides were dehydrated, mounted with Permout mounting medium (Fisher Scientific) and then observed under a bright-field microscope (Zeiss, Axiophot) or with polarizing lens. According to Junqueira *et al* (1979) picro-serius red staining may be considered specific for collagen type I, II and III detection when combined with polarized microscope. As a positive control, sections of the gland from which the nHSMGS was isolated were stained. The collagen type I appeared as thick yellow-red fibers, while the collagen type III as thin green fibers (Montes *et al*, 1991).

### *Plating of cells for cell viability and cell proliferation assays*

Human submandibular gland cell line (HSG) and Human foreskin fibroblasts (HFF) were maintained in Dulbecco's Modified Eagle's Medium (DMEM), containing 10% fetal bovine serum (FBS; Biofluids, Rockville, MD), and 1% of Gibco Antibiotic-Antimycotic. The cells, maintained at 37°C in a humidified 5% $CO_2$ and 95% air atmosphere incubator, were detached from 80% confluent plates with a solution of 0,05% trypsin, 0,02% versene (Biofluids, Rockville, MD) and re-suspended in fresh tissue culture media. For all experiments, HSG, HFF and a mixture 1:1 of the two cells types were plated at the density of $0.5\times10^5$ cells/slide.

The day of the plating, microslides with the scaffold sections were removed from -80°C. Each slide was placed inside a 100 × 15–mm plastic cell culture dish and washed with phosphate-buffered saline (PBS) + 5% of Gibco Antibiotic-Antimycotic. The washing buffer was substituted with the same culture medium used for the cell growth, then the dishes were placed in the incubator until seeding the cells. Once harvested the cells, the medium from each dish

containing the nHSMGS was removed and the cells were seeded on top of each slide. Samples were photographed under a phase contrast microscope (Leica DMIL, German) and incubated for 1h at 37°C in order to allow the cells to attach to the scaffold and spread. Culture media were then added in each dish for a final volume of 13 ml, and dishes were maintained at 37° C in a humidified 5% $CO_2$ and 95% air atmosphere incubator. Control experiments were performed following the same procedures either seeding cells directly on glass microslides without nHSMGS, or omitting cell seeding on slides containing the native scaffold. In all assays, each sample was examined in triplicate and each assay was repeated for three times.

***Cell proliferation evaluation and immunocytochemistry***

At day 4 of culture, Click-iT EdU Imaging Kit (C10337, Life technologies Inc.) was used to determinate the number of proliferating cells. EdU (5-ethynyl-2´-deoxyuridine) is a nucleoside analog of thymidine and is incorporated into DNA during active DNA synthesis. The kit is based on a click reaction, a copper-catalyzed covalent reaction between an azide (contained in the Alexa Fluor) and an alkyne (contained in the Edu). At day 3, samples were photographed at the phase contrast microscope and then, half of the culture media was removed and replaced with the same volume of complete culture media containing 20 μM Edu obtaining a final concentration of 10 μM. A negative control for Edu was obtained omitting the culture media+ Edu solution. After 24 hours, cells were fixed with 4% paraformaldehyde (PFA) + 5% of glucose, permeabilized with 0,5% of Triton X-100 and then incubated with the reaction cocktail. As indicated in the company protocol, cells were post-fixed with PFA and processed for immunohistochemistry and DNA staining. A solution with PBS+ BSA+ NGS was used as blocking solution and a rabbit anti-vimentin antibody (1:300; Abcam) was used in order to visualize the cell cytoplasm. A secondary Rhodamine-conjugated goat anti-rabbit antibody (1:200; Jackson ImmunoResearch Laboratories) was applied for 1h at room temperature in the dark; nuclei were stained with Hoechst 33342. Slides were then observed under a fluorescence microscope (Leica DM4000B), and randomly photographed.

### *Cell viability evaluation*

After 8 days of culture, samples were photographed using the phase contrast microscope and a LIVE/DEAD Viability/Cytotoxicity Kit (L3224, Life technologies Inc.) was used to evaluate cell vitality. The kit, based on plasma membrane integrity and esterase activity, is an easy two-color assay to determine viability of cells in a population. The two chemicals, Calcein-AM (indicating intracellular esterase activity with a green-fluorescent signal) and Ethidium homodimer-1 (indicating loss of plasma membrane integrity with a red-fluorescent signal) were used at the concentration of 1 and 2 μM respectively, to quickly discriminate live from dead cells by simultaneous staining. After staining, the slides were observed under a fluorescence microscope (Leica DM4000B) and randomly chosen images were taken for each slide.

## *Electron Microscopy*

### *Plating of cells for TEM and HRSEM*

nHSMGS was plated in 24-well plates (Costar, Corning) and incubated for 24h at 37°C in order to attach to the plate. Before seeding the cells, the scaffold was maintained with 200 μl of complete cell culture media. HSG and HFF cultured as previously described were harvested using a solution of 0,05% trypsin, 0,02% versene and then seeded on top of the scaffold with a density of $0.5\times10^5$ cell/well, with a final volume of 200 μl. Wells containing the scaffold alone and the cells alone were used as a controls. After 10 days of culture at 37°C in a humidified 5% $CO_2$ and 95% air atmosphere incubator the samples were processed for TEM and HRSEM as follows.

*Immunogold labeling at TEM for collagen type IV*

Samples for transmission electron microscopy were fixed with a solution of 4% paraformaldehyde (PFA) + 0,5% glutaraldehyde in 0,1 M of sodium cacodylate buffer for 4 hours at 4°C . After 1h washing samples were dehydrated through an increasing ethanol series and infiltrated and embedded in LR white resin. Sections of 80-90 nm in thickness were cut with an ultramicrotome and collected in nickel grids.

For the immunohistochemistry, the grids were hydrated with phosphate buffered saline (PBS) and then incubated with a blocking solution of PBS + 1% of bovine serum albumin (BSA) + 5% of normal goat serum (NGS) to block non-specific binding. Grids were then incubated over night at 4° C with the rabbit anti- collagen type IV primary antibody (Abcam ab6586) diluted 1:15 with the blocking solution. Controls were incubated respectively with a non immune rabbit serum or omitting the primary antibody. The following day the grids were rinsed in PBS and then incubated in the second blocking solution (PBS + 1% BSA) for 30 minutes. The goat anti-rabbit IgG conjugated with 15 nm gold particles secondary antibody (GE Healthcare, UK) diluted 1: 30 with PBS + 1% BSA was then applied for 1h at room temperature. After washing with PBS and distillated water the grids were stained with uranyl acetate and bismuth subnitrate, and observed with a transmission electron microscope (JEOL 100S at 80Kv). Pictures were randomly taken from at least two grids for each sample.

*Morphology at HRSEM*

Samples for scanning electron microscopy were fixed for 30 minutes with a solution of 4% paraformaldehyde (PFA) + 0,5 % glutaraldehyde in 0,1 M of sodium cacodylate buffer. Samples were then post-fixed with a mixture of 2% $OsO_4$ and 2,5% $K_3[Fe(CN)_6]$, dehydrated with an increasing series of acetones and then dried using a critical point dryer. Samples mounted on aluminum stubs, were coated with 20 nm of platinum and then observed with an Hitachi S4000 FEG HRSEM at 15–20 kV.

### *Statistic analysis*

All images were examined using ImageJ software (Wayne Resband, NIH, USA) and the obtained data were analyzed using an unpaired Student's t-test where P value < 0,05 represents significant differences between the two groups.

# RESULTS

## *Morphology of nHSMGS and cells*

The nHSMGS under the inverted light microscopy appears as a tangle of fibers (Fig. 19a). This network of fibers has been subsequently visualized in more details with the use of HRSEM (Fig. 19b), where fibers with different sizes are distinguishable (approximately 30-50 nm in diameter). The fiber arrangements appears comparable to that of fibers in the stroma of an intact gland (Fig. 19c).

The morphology of the native scaffold plus cells has been examined by phase contrast light and high resolution scanning electron microscopy. By light microscopy (Fig. 20), the connections between fibers and cells have been evaluated at day 0, 3 and 8 of culture. HSG and the mixture of HSG+ HFF always appear at higher cell density than HFF cells plated alone.

In order to investigate the fibers-cells interactions, an analysis of the utrastructure has been performed at day 10 by scanning electron microscopy (Fig. 21). Low magnification images display the scaffold as an uniform surface on which the cells lie. HFF appear widespread on the matrix (c), while HSG and the combined HSG+HFF are more aggregated (b and d). No cells are observed in the nHSMGS used as a negative control (a). High magnifications allow to appreciate the network of fibers and cells anchored by means of several processes (Fig. 22).

## *Collagen detection*

Fibers of collagen type I and III are detected in the slides stained with picro-sirius red observed under a polarized light microscope (Fig. 23). In nHSMGS (c, d), even if fibers appear disorganized, both collagen types are present. The positive scaffold control (i.e. the intact salivary gland; Fig 23a, b) shows strongly stained collagen type I in all the stroma, while type III collagen is restricted to fibers surrounding acini and ducts.

### *Immunolabeling for collagen Type IV*

Collagen type IV is detected (Fig. 24) in the intact glands in the basal lamina surrounding acini and ducts (a, b). In nHSMGS (c, d, e) a basal lamina is not detectable, but gold particles are observed in amorphous masses among the electron dense fibers which usually are not stained. No gold particles are observed in the negative controls (f, g).

### *Cell proliferation*

Cell proliferation has been evaluated after 4 days of culture using the click Edu assay. The green signal indicating cell proliferation appears co-localized with the blue (Hoechst) in numerous nuclei of cells cultured on nHSMGS and on glass (Fig. 25). HSG (b) and HSG+HFF mixture (d) cultured on nHSMGS show more proliferating cells than those cultured on glass (microslides without scaffold). Controls: no proliferating cells are observed in the nHSMGS alone (a), while cells cultured in glass (e, f, g) show a discrete percentage of proliferating cells. Fig h represents the negative control for the Edu, where green nuclei are not observed.

Statistical analysis (Fig. 26a) confirms an increased percentage of proliferating cells (% of Edu positive cells/ 100 $\mu m^2$) in HSG ($P < 0,01$) and HSG+HFF ($P < 0,05$) cultured in nHSMGS with respect to the cells cultured on glass, while no differences are observed for HFF.

### *Cell viability*

A live and dead assay has been performed after 8 days of culture in order to evaluate cell viability. The cells HSG, HFF and HSG+HFF seeded on the nHSMGS (Fig. 27 b, c, d) show all a high percentage of live cells (green cytoplasm) as well as the control cells cultured without scaffold (e, f, g). Conversely, only a few red nuclei corresponding to the dead cells are detected. No cells are observed in the nHSMGS (a).

Statistical analysis demonstrates no significant differences in cell viability between the cells cultured in the nHSMGS and the cells cultured on glass (Fig. 26b).

# DISCUSSION

The results of the experiments show that the stroma of human submandibular gland takes no evident damages after cell detachment. In fact the appearance and the organization of the collagen fibers of nHSMGS correspond, both in light and electron microscopy, very well to those in the intact gland. Moreover, the staining of the three types of collagen indicates that the native scaffold maintains them even after enzymatic treatment: this represents an advantage with respect to other scaffolds which need to be supplemented with ECM to improve functionality. Of course it is necessary to demonstrate the presence of many other ECM proteins such as fibronectin and laminin before stating that this scaffold possesses the entire correct protein outfit. In intact glands, collagen type I is present in the capsule, in septa, and in the interstitium among acini and ducts, while collagen type III, often co-localized with the type I, is chiefly concentrated around acini and ducts (Goicovich *et al*, 2003; Kumagai and Sato, 2003 ; Ueda *et al*, 2009). The histochemical staining in native scaffold suggests that their spatial arrangement also is maintained: thicker masses stained for type I collagen probably represent what remains of septa, while the thinner filaments stained for type III collagen surround circular spaces where likely acini and ducts were attached. Collagen type IV, a typical component of basal lamina, in intact salivary glands is localized by immunolabeling in the basal lamina surrounding acini and ducts. It results still detectable in the nHSMGS after cell detachment but its localization is less precisely defined. Although a basal lamina is not recognizable in native scaffold at the electron microscopy level, the collagen type IV labeling appears more concentrated in amorphous areas but not in the electron-dense fibers, suggesting that basal lamina-like structures will be reorganized in these areas.

In order to verify the qualities of this matrix, cells have been seeded on the nHSMGS and their behavior has been evaluated. The ability of cells to relate with this matrix is showed by images at the phase contrast microscope during the culture and especially by HRSEM micrographs after 10 days of culture where clear processes that anchor cells to the fibers are visible. These results, even if based on the mere observation, are a good starting point to reinforce the

thought that this native matrix may represent a good substrate in which salivary cells can grow. This assumption is supported by the data of cell proliferation and viability assays. The results demonstrate in fact that the cells are not just anchored to the matrix, but also proliferating (after 4 days of culture) and that after 8 days the majority of the cells are still alive. Moreover, the more abundant proliferating cells in nHSMGS rather than in glass confirm the assumption that cell activities are strictly influenced by the surrounding microenvironment and that the same cell type can display different behavior depending on the used matrix (Aframian *et al*, 2002; Maria *et al*, 2011a, Yamada *et al*, 2012). The three-dimensionality of the native scaffold, the presence of ECM proteins, and probably the presence of other factors may positively influence cell behavior.

In conclusion, the results of these experiments preliminarily delineate some properties of the native scaffold obtained from intact salivary glands and encourage its use as autologous substrate for expanding salivary gland cells and obtain artificial parenchyma to be implanted in patients with damaged salivary glands.

## REFERENCES


Acuña-Castroviejo D, Escames G, Venegas C, Díaz-Casado ME, Lima-Cabello E, López LC, Rosales-Corral S, Tan DX, Reiter RJ. Extrapineal melatonin: sources, regulation, and potential functions. Cell Mol Life Sci. 2014 Aug;71(16):2997-3025.

Abdolsamadi H, Goodarzi MT, Ahmadi Motemayel F, Jazaeri M, Feradmal J, Zarabadi M, Hoseyni M, Torkzaban P. Reduction of Melatonin Level in Patients with Type II Diabetes and Periodontal Diseases.J Dent Res Dent Clin Dent Prospects. 2014 Summer; 8(3):160-165

Aframian DJ, Cukierman E, Nikolovski J, Mooney DJ, Yamada KM, Baum BJ. The growth and morphological behavior of salivary epithelial cells on matrix protein-coated biodegradable substrata. Tissue Eng. 2000 Jun;6(3):209-216.

Aframian DJ, Tran SD, Cukierman E, Yamada KM, Baum BJ. Absence of tight junction formation in an allogeneic graft cell line used for developing an engineered artificial salivary gland. Tissue Eng. 2002 Oct;8(5):871-878.

Almughrabi OM, Marzouk KM, Hasanato RM, Shafik SS. Melatonin levels in periodontal health and disease. J Periodontal Res. 2013 Jun;48(3):315-321.

Ambudkar IS. $Ca^{2+}$ signaling and regulation of fluid secretion in salivary gland acinar cells. Cell Calcium. 2014 Jun;55(6):297-305.

Anderson L.C. Hormonal Regulation of Salivary Glands, with Particular Reference to Experimental Diabetes. Garrett JR, Ekström J, Anderson LC (eds): Glandular Mechanisms of Salivary Secretion.Front Oral Biol. Basel, Karger, 1998, vol 10, pp 200-221

Anderson LC, Garrett JR, Proctor GB. Morphological effects of sympathetic nerve stimulation on rat parotid glands 3-4 weeks after the induction of streptozotocin diabetes. Arch Oral Biol. 1990;35(10):829-838.

Aneiros-Fernandez J, Arias-Santiago S, Arias-Santiago B, Herrero-Fernández M, Carriel V, Aneiros-Cachaza J, López-Valverde A, Cutando-Soriano A. MT1

melatonin receptor expression in Warthin's tumor. Pathol Oncol Res. 2013 Apr;19(2):247-250.

Aras HC, Ekström J. Melatonin-evoked in vivo secretion of protein and amylase from the parotid gland of the anaesthetised rat. J Pineal Res. 2008 Nov;45(4):413-421.

Arias-Santiago S, Aneiros-Fernández J, Arias-Santiago B, Girón-Prieto MS, Caba-Molina M, López-Valverde A, Aneiros-Cachaza J, Campos A, Cutando A. MTNR1A receptor expression in normal and pathological human salivary glands. Anticancer Res. 2012 Nov;32(11):4765-4771.

Barnes VM, Kennedy AD, Panagakos F, Devizio W, Trivedi HM, Jönsson T, Guo L, Cervi S, Scannapieco FA. Global metabolomic analysis of human saliva and plasma from healthy and diabetic subjects, with and without periodontal disease. PLoS One. 2014 Aug 18;9(8):e105181.

Baum BJ. Principles of saliva secretion. Ann N Y Acad Sci. 1993 Sep 20;694:17-23.

Ben-Aryeh H, Serouya R, Kanter Y, Szargel R, Laufer D. Oral health and salivary composition in diabetic patients. J Diabetes Complications. 1993 Jan-Mar;7(1):57-62.

Caldeira EJ, Camilli JA, Cagnon VH. Stereology and ultrastructure of the salivary glands of diabetic Nod mice submitted to long-term insulin treatment. Anat Rec A Discov Mol Cell Evol Biol. 2005 Oct;286(2):930-937.

Campbell CB, Cukierman E, Artym VV. 3-D extracellular matrix from sectioned human tissues. Curr Protoc Cell Biol. 2014 Mar 3;62:Unit 19.16.1-20.

Cantara SI, Soscia DA, Sequeira SJ, Jean-Gilles RP, Castracane J, Larsen M. Selective functionalization of nanofiber scaffolds to regulate salivary gland epithelial cell proliferation and polarity. Biomaterials. 2012 Nov;33(33):8372-8382.

Carda C, Mosquera-Lloreda N, Salom L, Gomez de Ferraris ME, Peydró A. Structural and functional salivary disorders in type 2 diabetic patients. Med Oral Patol Oral Cir Bucal 2006; 1: 309-314.

Castle D and Castle A. Intracellular transport and secretion of salivary proteins. Crit Rev Oral Biol Med. 1998;9(1):4-22.

Castle JD and Castle AM. Two regulated secretory pathways for newly synthesized parotid salivary proteins are distinguished by doses of secretagogues. J Cell Sci. 1996 Oct;109 ( Pt 10):2591-2599.

Cengiz Mİ, Cengiz S, Wang HL. Melatonin and oral cavity. Int J Dent. 2012;2012:491872.

Chambers MS, Garden AS, Kies MS, Martin JW. Radiation-induced xerostomia in patients with head and neck cancer: pathogenesis, impact on quality of life, and management. Head Neck. 2004 Sep;26(9):796-807.

Chan KM, Chao J, Proctor GB, Garrett JR, Shori DK, Anderson LC. Tissue kallikrein and tonin levels in submandibular glands of STZ-induced diabetic rats and the effects of insulin. Diabetes. 1993 Jan;42(1):113-117.

Chen MH, Chen RS, Hsu YH, Chen YJ, Young TH. Proliferation and phenotypic preservation of rat parotid acinar cells. Tissue Eng. 2005 Mar-Apr;11(3-4):526-534.

Cutando A, Gómez-Moreno G, Villalba J, Ferrera MJ, Escames G, Acuña-Castroviejo D. Relationship between salivary melatonin levels and periodontal status in diabetic patients. J Pineal Res. 2003 Nov;35(4):239-244.

Cutler LS (1989). Functional differentiation of salivary glands. In: Forte JG, Rauner BB, eds. Handbook of physiology, Sect. 6: The gastrointestinal system. Am Physiological Soc: Bethesda, MD, pp. 93–105.

Dawes C and Wood CM. The contribution of oral minor mucous gland secretions to the volume of whole saliva in man. Arch Oral Biol. 1973 Mar; 18(3): 337-342.

Dawes C. Physiological factors affecting salivary flow rate, oral sugar clearance, and the sensation of dry mouth in man. J Dent Res. 1987 Feb;66 Spec No:648-653.

Deepa T and Thirrunavukkarasu N. Saliva as a potential diagnostic tool. Indian J Med Sci. 2010 Jul;64(7):293-306.

Denny PC, Ball WD, Redman RS. Salivary glands: a paradigm for diversity of gland development. Crit Rev Oral Biol Med. 1997;8(1):51-75.

Dodds MW and Dodds AP. Effects of glycemic control on saliva flow rates and protein composition in non-insulin-dependent diabetes mellitus. Oral Surg Oral Med Oral Pathol Oral Radiol Endod. 1997 Apr;83(4):465-470.

Dodds MW, Yeh CK, Johnson DA. Salivary alterations in type 2 (non-insulin-dependent) diabetes mellitus and hypertension. Community Dent Oral Epidemiol. 2000 Oct;28(5):373-381.

Dodds MW, Johnson DA, Yeh CK. Health benefits of saliva: a review. J Dent. 2005 Mar;33(3):223-233.

Donath K. and Seifert G. Ultrastructural studies of the parotid glands in sialadenosis. Virchows Archiv A Pathol Anat Histol 1975; 365: 119-135.

Dubocovich ML and Markowska M. Functional MT1 and MT2 melatonin receptors in mammals. Endocrine. 2005 Jul;27(2):101-110.

Ekström J. and Khosravani N. 2011. Regulatory mechanisms and salivary gland functions. Patrick J. Bradley, Orlando Guntinas-Lichius, Salivary Gland Disorders: Diagnosis and Management. - Stuttgart, Germany : Georg Thieme Verlag. 2011 ; pp 10-18

Fedirko NV, Kruglikov IA, Kopach OV, Vats JA, Kostyuk PG, Voitenko NV. Changes in functioning of rat submandibular salivary gland under streptozotocin-induced diabetes are associated with alterations of Ca2+ signaling and Ca2+ transporting pumps. Biochim Biophys Acta. 2006 Mar;1762(3):294-303.

Fox PC. Xerostomia: recognition and management. Dent Assist. 2008 Sep-Oct;77(5):18, 20, 44-48.

Galano A, Tan DX, Reiter RJ. Melatonin as a natural ally against oxidative stress: a physicochemical examination. J Pineal Res. 2011 Aug;51(1):1-16.

Goicovich E, Molina C, Pérez P, Aguilera S, Fernández J, Olea N, Alliende C, Leyton C, Romo R, Leyton L, González MJ. Enhanced degradation of proteins of the basal lamina and stroma by matrix metalloproteinases from the salivary

glands of Sjögren's syndrome patients: correlation with reduced structural integrity of acini and ducts. Arthritis Rheum. 2003 Sep;48(9):2573-84.

Guggenheimer J and Moore PA. Xerostomia: etiology, recognition and treatment. J Am Dent Assoc. 2003 Jan;134(1):61-69.

Güne S, Yilmaz S, Karalezli A, Aktaş A. Quantitative and visual evaluation of salivary and thyroid glands in patients with primary Sjögren's syndrome using salivary gland scintigraphy: relationship with clinicopathological features of salivary, lacrimal and thyroid glands. Nucl Med Commun. 2010 Jul;31(7):666-672.

Hakkinen KM, Harunaga JS, Doyle AD, Yamada KM. Direct comparisons of the morphology, migration, cell adhesions, and actin cytoskeleton of fibroblasts in four different three-dimensional extracellular matrices. Tissue Eng Part A. 2011 Mar;17(5-6):713-724.

Hand AR and Weiss RE. Effects of streptozotocin-induced diabetes on the rat parotid gland. Lab Invest. 1984 Oct;51(4):429-440.

Hevia D, Sainz RM, Blanco D, Quirós I, Tan DX, Rodríguez C, Mayo JC. Melatonin uptake in prostate cancer cells: intracellular transport versus simple passive diffusion. J Pineal Res. 2008 Oct;45(3):247-257.

Hevia D, González-Menéndez P, Quiros-González I, Miar A, Rodríguez-García A, Tan DX, Reiter RJ, Mayo JC, Sainz RM. Melatonin uptake through glucose transporters: a new target for melatonin inhibition of cancer. J Pineal Res. 2015 Mar;58(2):234-250.

Huang AY, Castle AM, Hinton BT, Castle JD. Resting (basal) secretion of proteins is provided by the minor regulated and constitutive-like pathways and not granule exocytosis in parotid acinar cells. J Biol Chem. 2001 Jun 22;276(25):22296-306.

Huoh KC, Eisele DW. Etiologic factors in sialolithiasis. Otolaryngol Head Neck Surg. 2011 Dec;145(6):935-939.

Isola M, Solinas P, Proto E, Cossu M, Lantini MS. Reduced statherin reactivity of human submandibular gland in diabetes. Oral Dis. 2011a Mar;17(2):217-220.

Isola M, Lantini M, Solinas P, Diana M, Isola R, Loy F, Cossu M. Diabetes affects statherin expression in human labial glands. Oral Dis. 2011b Oct;17(7):685-689.

Isola M, Cossu M, Diana M, Isola R, Loy F, Solinas P, Lantini MS. Diabetes reduces statherin in human parotid: immunogold study and comparison with submandibular gland. Oral Dis. 2012 May;18(4):360-364.

Jang SI, Ong HL, Gallo A, Liu X, Illei G, Alevizos I. Establishment of functional acinar-like cultures from human salivary glands. J Dent Res. 2015 Feb;94(2):304-311.

Jeong SY, Kim HW, Lee SW, Ahn BC, Lee J. Salivary gland function 5 years after radioactive iodine ablation in patients with differentiated thyroid cancer: direct comparison of pre- and postablation scintigraphies and their relation to xerostomia symptoms. Thyroid. 2013 May;23(5):609-616.

Joraku A, Sullivan CA, Yoo JJ, Atala A. Tissue engineering of functional salivary gland tissue. Laryngoscope. 2005 Feb;115(2):244-248.

Junqueira LC, Bignolas G, Brentani RR. Picrosirius staining plus polarization microscopy, a specific method for collagen detection in tissue sections. Histochem J. 1979 Jul;11(4):447-455.

Kagami H, Wang S, Hai B. Restoring the function of salivary glands. Oral Dis. 2008 Jan;14(1):15-24.

Kaplan MD, Baum BJ. The functions of saliva. Dysphagia. 1993;8(3):225-229.

Kaufman E, Lamster IB. The diagnostic applications of saliva--a review. Crit Rev Oral Biol Med. 2002;13(2):197-212.

Kumagai M and Sato I. Immunolocalization of fibronectin and collagen types I and III in human fetal parotid and submandibular glands. Cells Tissues Organs. 2003;173(3):184-190.

Kvetnoy IM. Extrapineal melatonin: location and role within diffuse neuroendocrine system. Histochem J. 1999 Jan;31(1):1-12.

Laakso ML, Porkka-Heiskanen T, Alila A, Stenberg D, Johansson G Correlation between salivary and serum melatonin: dependence on serum melatonin levels. J Pineal Res. 1990;9(1):39-50.

Lawrence HP. Salivary markers of systemic disease: noninvasive diagnosis of disease and monitoring of general health. J Can Dent Assoc. 2002; 68(3):170-174.

Leite RS, Marlow NM, Fernandes JK. Oral health and type 2 diabetes. Am J Med Sci. 2013 Apr;345(4):271-273.

Loe H. Periodontal disease. The sixth complication of diabetes mellitus. Diabetes care. 1993; 16(1): 329–334.

Loy F, Diana M, Isola R, Solinas P, Isola M, Conti G, Lantini MS, Cossu M, Riva A, Ekström J. Morphological evidence that pentagastrin regulates secretion in the human parotid gland. J Anat. 2012 May;220(5):447-453.

Loy F, Isola M, Isola R, Lilliu MA, Solinas P, Conti G, Godoy T, Riva A, Ekström J. The antipsychotic amisulpride: ultrastructural evidence of its secretory activity in salivary glands. Oral Dis. 2014 Nov;20(8):796-802.

Maria OM, Maria O, Liu Y, Komarova SV, Tran SD. Matrigel improves functional properties of human submandibular salivary gland cell line. Int J Biochem Cell Biol. 2011a Apr;43(4):622-631.

Maria OM, Zeitouni A, Gologan O, Tran SD. Matrigel improves functional properties of primary human salivary gland cells. Tissue Eng Part A. 2011b May;17(9-10):1229-1238.

Martin TF. Stages of regulated exocytosis. Trends Cell Biol. 1997 Jul;7(7):271-6.

Mata AD, Marques D, Rocha S, Francisco H, Santos C, Mesquita MF, Singh J. Effects of diabetes mellitus on salivary secretion and its composition in the human. Mol Cell Biochem 2004; 261: 137-142.

Mattei G, Di Patria, Tirella A, Alaimo A, Elia G, Corti A, Paolicchi A, Ahluwalia A. Mechanostructure and composition of highly reproducible decellularized liver matrices. Acta Biomater. 2014 Feb;10(2):875-882.

Mauriz JL, Collado PS, Veneroso C, Reiter RJ, González-Gallego J. A review of the molecular aspects of melatonin's anti-inflammatory actions: recent insights and new perspectives. J Pineal Res. 2013 Jan;54(1):1-14.

Miletich I. Introduction to salivary glands: structure, function and embryonic development. Tucker A.S. and Miletich I. (eds), Salivary Glands. Development, adaptation and disease. Front Oral Biol. Basel, Karger, 2010, vol 14, pp 1-20

Montes GS, Junqueira LC. The use of the Picrosirius-polarization method for the study of the biopathology of collagen. Mem Inst Oswaldo Cruz. 1991;86 Suppl 3:1-11.

Nagler RM, Laufer D. Tumors of the major and minor salivary glands: review of 25 years of experience. Anticancer Res. 1997 Jan-Feb;17(1B):701-707.

Nagy K, Szlávik V, Rácz G, Ovári G, Vág J, Varga G. Human submandibular gland (HSG) cell line as a model for studying salivary gland Ca2+ signalling mechanisms. Acta Physiol Hung. 2007 Dec;94(4):301-313.

Palade G. Intracellular aspects of the process of protein synthesis. Science. 1975 Aug 1;189(4200):347-58.

Pink R, Simek J, Vondrakova J, Faber E, Michl P, Pazdera J, Indrak K. Saliva as a diagnostic medium. Biomed Pap Med Fac Univ Palacky Olomouc Czech Repub. 2009 Jun;153(2):103-110.

Redman RS (1987). Development of the salivary glands. In: Sreebny LM, ed. The salivary system. CRC Press: Boca Raton, FL, pp. 2–17.

Reiter RJ, Rosales-Corral SA, Liu XY, Acuna-Castroviejo D, Escames G, Tan DX. Melatonin in the oral cavity: physiological and pathological implications. J Periodontal Res. 2015 Feb;50(1):9-17.

Riva A, Loy F, Isola R, Isola M, Conti G, Perra A, Solinas P, Testa Riva F. New findings on 3-D microanatomy of cellular structures in human tissues and organs. An HRSEM study. Eur J Histochem. 2007;51 Suppl 1:53-58.

Riva A., Lantini M.S. and Testa Riva F. Normal human salivary glands. Riva A. and Motta P.M., (eds), Ultrastructure of the extraparietal glands of the digestive tract. 1990. Kluwer Academic Publishers pp. 53-74.

Saleh J, Figueiredo MA, Cherubini K, Salum FG. Salivary hypofunction: An update on aetiology, diagnosis and therapeutics. Arch Oral Biol. 2015 Feb;60(2):242-255.

Shimozuma M, Tokuyama R, Tatehara S, Umeki H, Ide S, Mishima K, Saito I, Satomura K. Expression and cellular localization of melatonin-synthesizing enzymes in rat and human salivary glands. Histochem Cell Biol. 2011 Apr;135(4):389-396

Shirasuna K, Sato M, Miyazaki T. A neoplastic epithelial duct cell line established from an irradiated human salivary gland. Cancer. 1981 Aug 1;48(3):745-752.

Soscia DA, Sequeira SJ, Schramm RA, Jayarathanam K, Cantara SI, Larsen M, Castracane J. Salivary gland cell differentiation and organization on micropatterned PLGA nanofiber craters. Biomaterials. 2013 Sep;34(28):6773-6784.

Styskal J, Van Remmen H, Richardson A, Salmon AB. Oxidative stress and diabetes: what can we learn about insulin resistance from antioxidant mutant mouse models? Free Radic Biol Med. 2012 Jan 1;52(1):46-58.

Südhof TC. The synaptic vesicle cycle. Annu Rev Neurosci. 2004;27:509-47.

Tandler B, Phillips CJ. Structure of serous cells in salivary glands. Microsc Res Tech. 1993 Sep 1;26(1):32-48.

Tandler B. Salivary Glands and the secretory process. In: A textbook of oral biology. JH Shaw, EA Sweeney, CC Cappuccino, SM Meller (eds), Philadelphia: WB Saunders, 547-592, 1978.

Tooze SA. Biogenesis of secretory granules in the trans-Golgi network of neuroendocrine and endocrine cells. Biochim Biophys Acta. 1998 Aug 14;1404(1-2):231-244.

Tran H, Pankov R, Tran SD, Hampton B, Burgess WH, Yamada KM. Integrin clustering induces kinectin accumulation. J Cell Sci. 2002 May 15;115(Pt 10):2031-2040.

Tran SD, Wang J, Bandyopadhyay BC, Redman RS, Dutra A, Pak E, Swaim WD, Gerstenhaber JA, Bryant JM, Zheng C, Goldsmith CM, Kok MR, Wellner RB, Baum BJ. Primary culture of polarized human salivary epithelial cells for use in developing an artificial salivary gland. Tissue Eng. 2005 Jan-Feb;11(1-2):172-181.

Ueda K, Shimizu O, Oka S, Saito M, Hide M, Matsumoto M. Distribution of tenascin-C, fibronectin and collagen types III and IV during regeneration of rat submandibular gland. Int J Oral Maxillofac Surg. 2009 Jan;38(1):79-84.

Venegas C, García JA, Escames G, Ortiz F, López A, Doerrier C, García-Corzo L,López LC, Reiter RJ, Acuña-Castroviejo D. Extrapineal melatonin: analysis of its subcellular distribution and daily fluctuations. J Pineal Res. 2012 Mar;52(2):217-227.

Walters NJ, Gentleman E. Evolving insights in cell-matrix interactions: elucidating how non-soluble properties of the extracellular niche direct stem cell fate. Acta Biomater. 2015 Jan 1;11:3-16.

Wang S, Cukierman E, Swaim WD, Yamada KM, Baum BJ. Extracellular matrix protein-induced changes in human salivary epithelial cell organization and proliferation on a model biological substratum. Biomaterials. 1999 Jun;20(11):1043-1049.

Yamada Y, Hozumi K, Aso A, Hotta A, Toma K, Katagiri F, Kikkawa Y, Nomizu M. Laminin active peptide/agarose matrices as multifunctional biomaterials for tissue engineering. Biomaterials. 2012 Jun;33(16):4118-4125.

Zarain-Herzberg A, García-Rivas G, Estrada-Avilés R. Regulation of SERCA pumps expression in diabetes. Cell Calcium. 2014 Nov;56(5):302-310.

Zhao B, Sun X, Li X, Yang Q, Li Y, Zhang Y, Li B, Ma X. Improved preparation of acellular nerve scaffold and application of PKH26 fluorescent labeling combined with in vivo fluorescent imaging system in nerve tissue engineering. Neurosci Lett. 2013 Nov 27;556:52-57.

| Function | Salivary component(s) mediating function |
|---|---|
| Mucosal protection | Mucins, basic proline-rich glycoprotein, epidermal growth factor |
| pH maintenance | Bicarbonate, histatins |
| Microbial control | Histatins, sIgA, lysozyme, lactoferrin, salivary peroxidase, fibronectin |
| Remineralization of teeth | Statherin, proline-rich proteins |
| Alimentation, bolus formation, translocation | Mucin, $H_2O$ |
| Digestion | Various hydrolytic enzymes: lingual lipase, DNase, RNase, amylase |
| Taste mediation (as a solvent and delivery system) | $H_2O$ |

Fig. 1. Functional properties of saliva. (source: Kaplan and Baum, 1993).

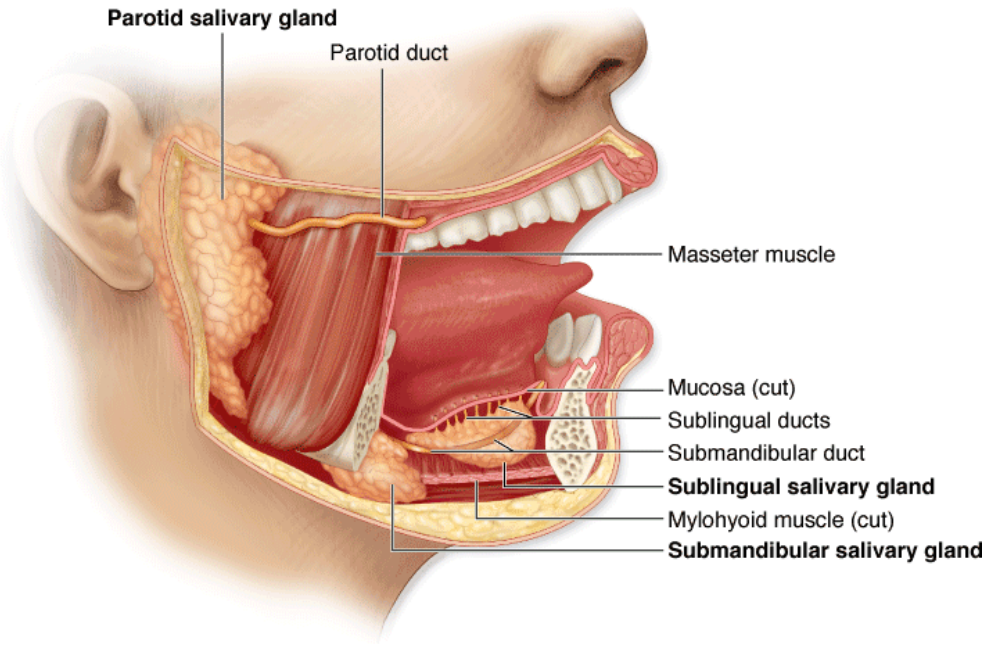


Fig. 2. Major salivary gland location. (source: Mascher AL: Junqueira's Basic Histology: Text and Atlas 12th Edition).

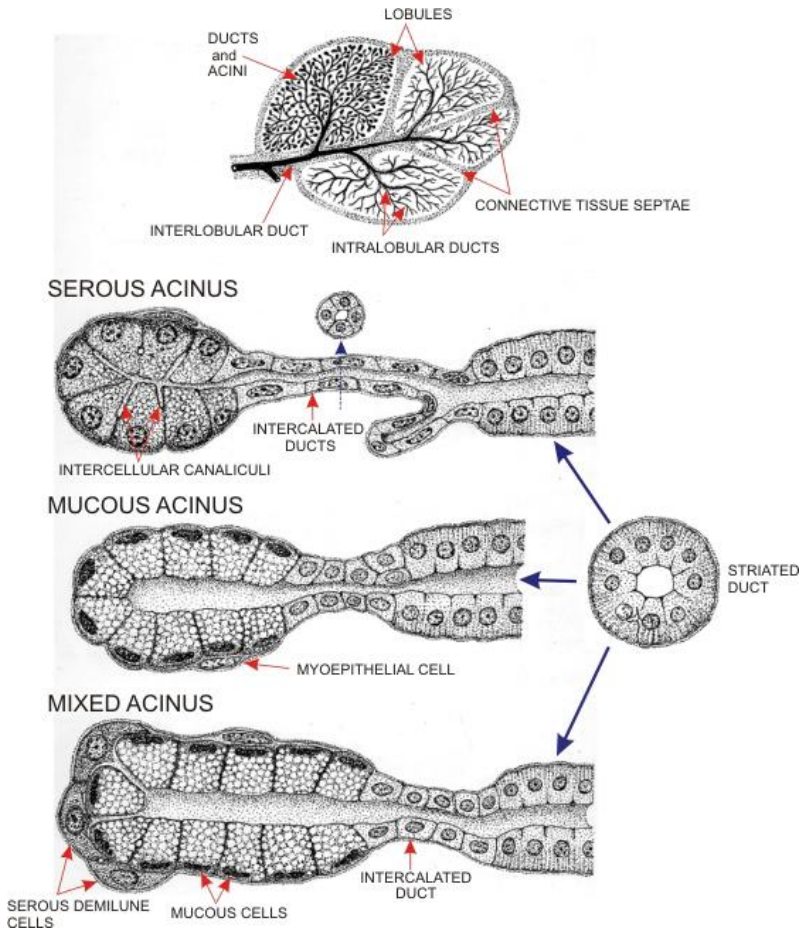


Fig. 3. Structure of the salivary glands and different types of acini and ducts. (source: Histology Atlas, Yves Clermont, Michael Lalli & Zsuzsanna Bencsath-Makkai).

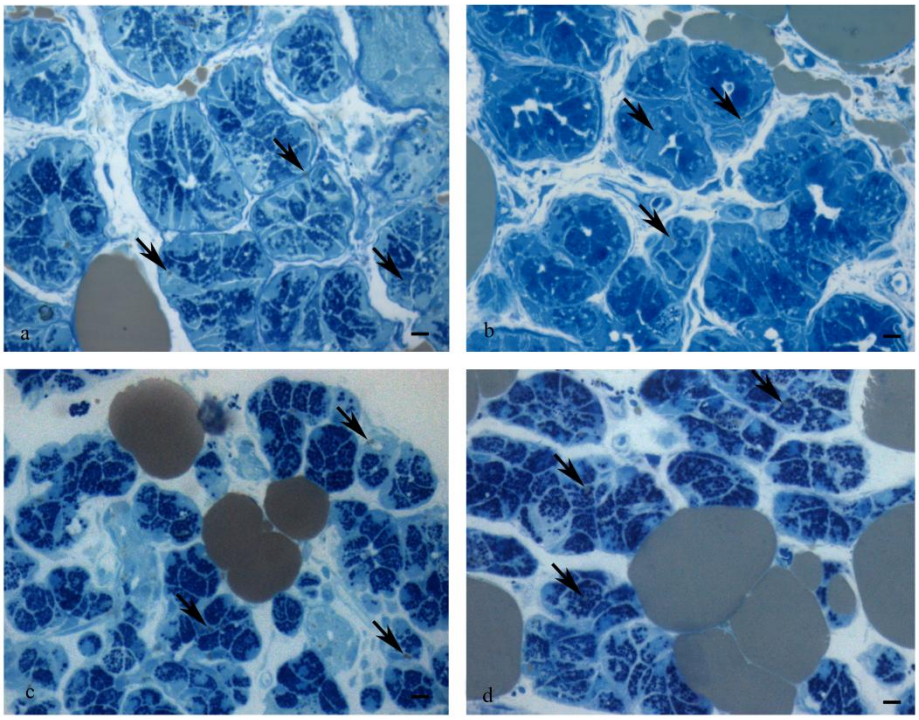


Fig. 4. Light microscopy (LM) images of submandibular (a, b) and parotid glands (c, d) stained with toluidine blue. Apparently the morphology of diabetic (b, d) is very similar when compared to non-diabetic glands (a, c). Intracellular lipid droplets are observed in all samples (arrows). Bar = 10 μm

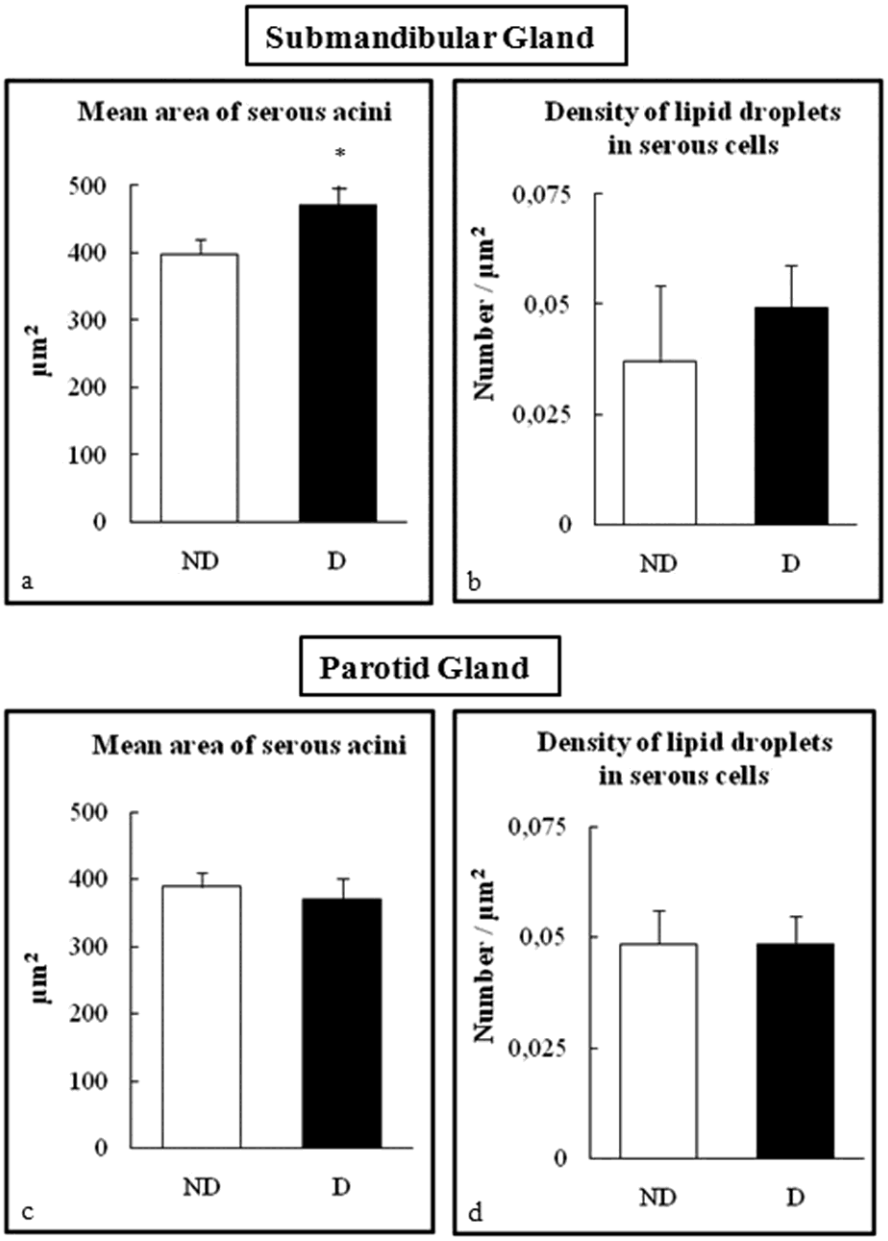


Fig. 5. Morphometrical evaluation of LM images. The mean area of serous acini in submandibular (a) results significantly larger in diabetic (D) than non-diabetic (ND), while no differences are reported in parotid (c) glands. In both glands, no statistically significant difference is observed in the lipid droplet density (b, d). * $P < 0,05$

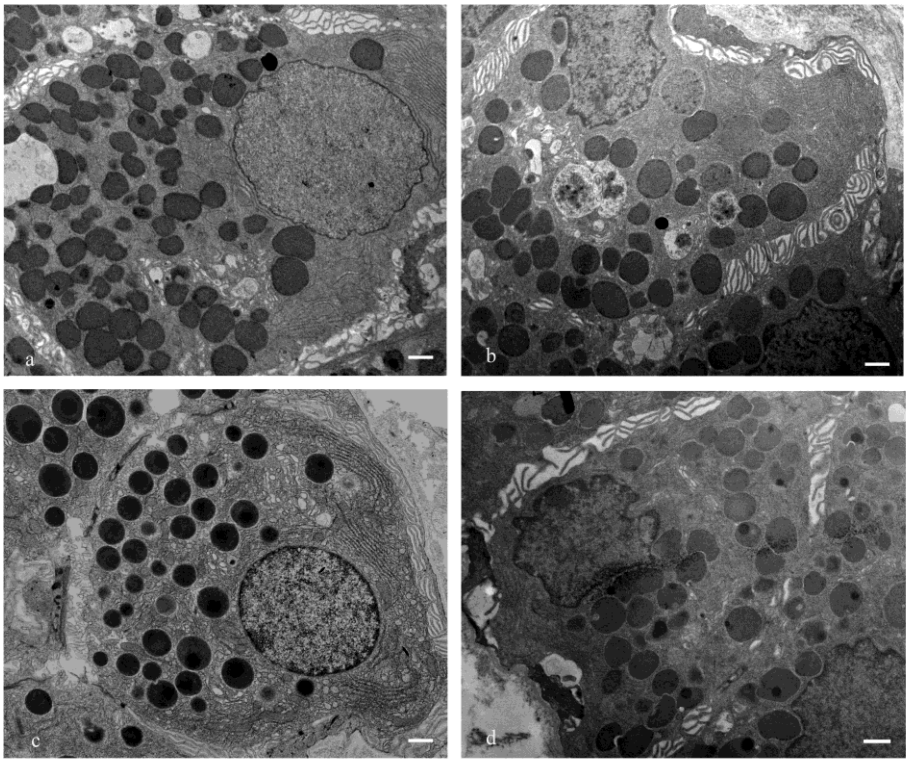


Fig. 6. Transmission electron microscopy (TEM) images of submandibular (a, b) and parotid (c, d) serous cells post-fixed with osmium tetroxide. Cell membranes and organelles show an apparently normal aspect in both diabetics (b, d) and non-diabetics (a, c). Bar = 1 μm

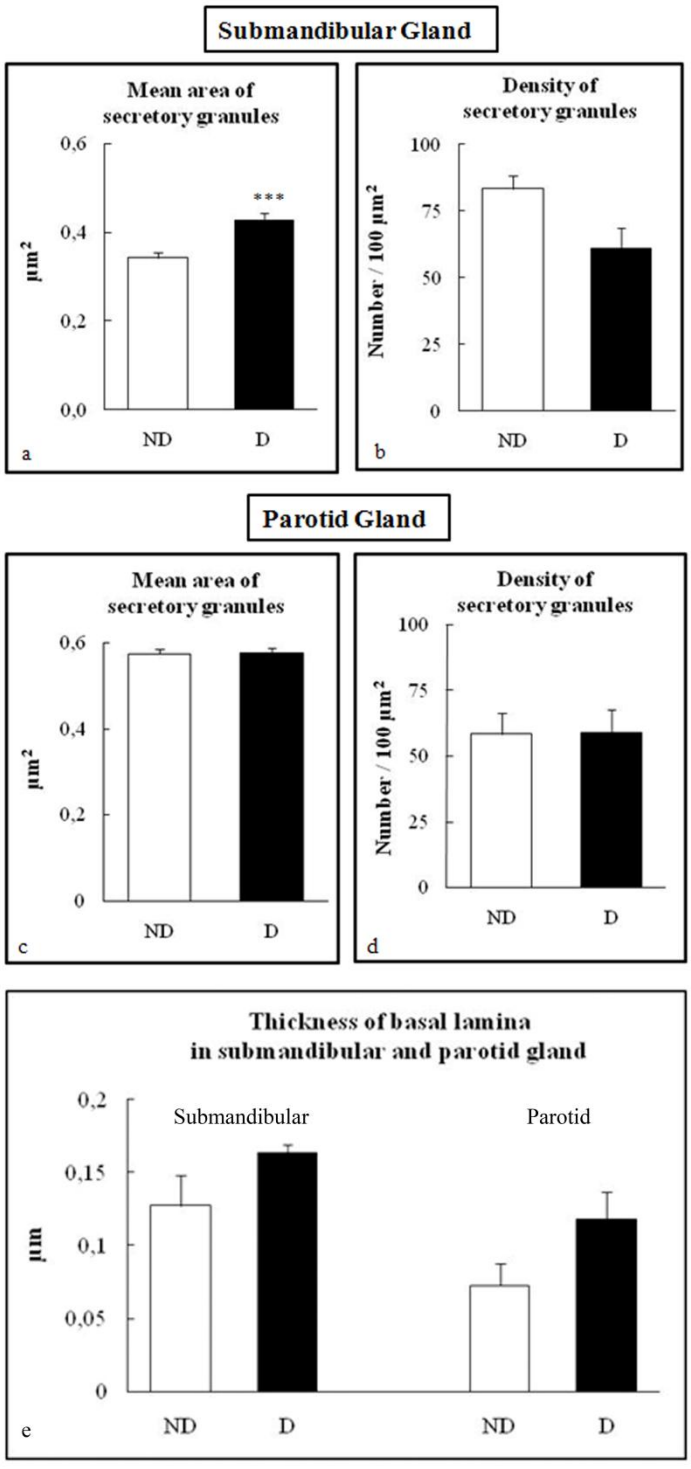


Fig. 7. Morphometrical evaluation of TEM images. The mean area of secretory granules in submandibular glands (a) results significantly larger in diabetics (D) than in non-diabetics (ND), while no difference is reported in parotid glands (c). No significant difference is observed in the secretory granules density (b, d) between diabetics and non-diabetics, but in submandibular glands (b) there is a tendency to decrease in diabetics. No significant difference is observed in the thickness of basal lamina (e). *** $P < 0,001$

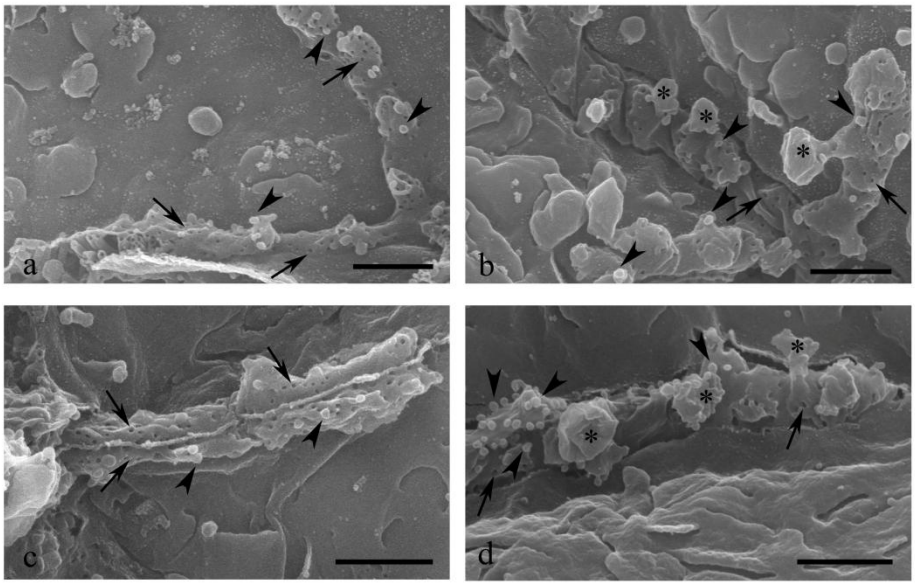


Fig. 8. High resolution scanning electron microscopy (HRSEM) images of luminal membranes bordering intercellular canaliculi in submandibular (a, b) and parotid glands (c, d) of diabetics (b, d) and non-diabetics (a, c). Note the holes corresponding to the base of microvilli (arrows), the microbuds (arrowheads) corresponding to apical vesicles, and the large protrusions (asterisks) corresponding to docked granules. Bar 1 μm.

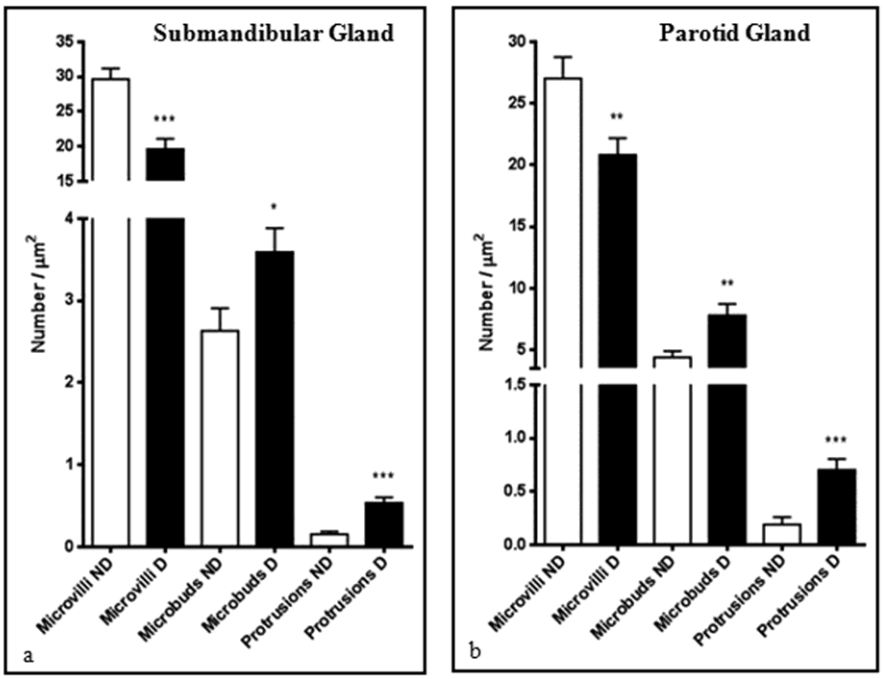


Fig. 9. Morphometrical evaluation of HRSEM images. The density of microvilli results significantly decreased, while that of microbuds and protrusions significantly increased in diabetic (D) submandibular (a) and parotid (b) glands. * $P < 0,05$; ** $P < 0,01$; *** $P < 0,001$

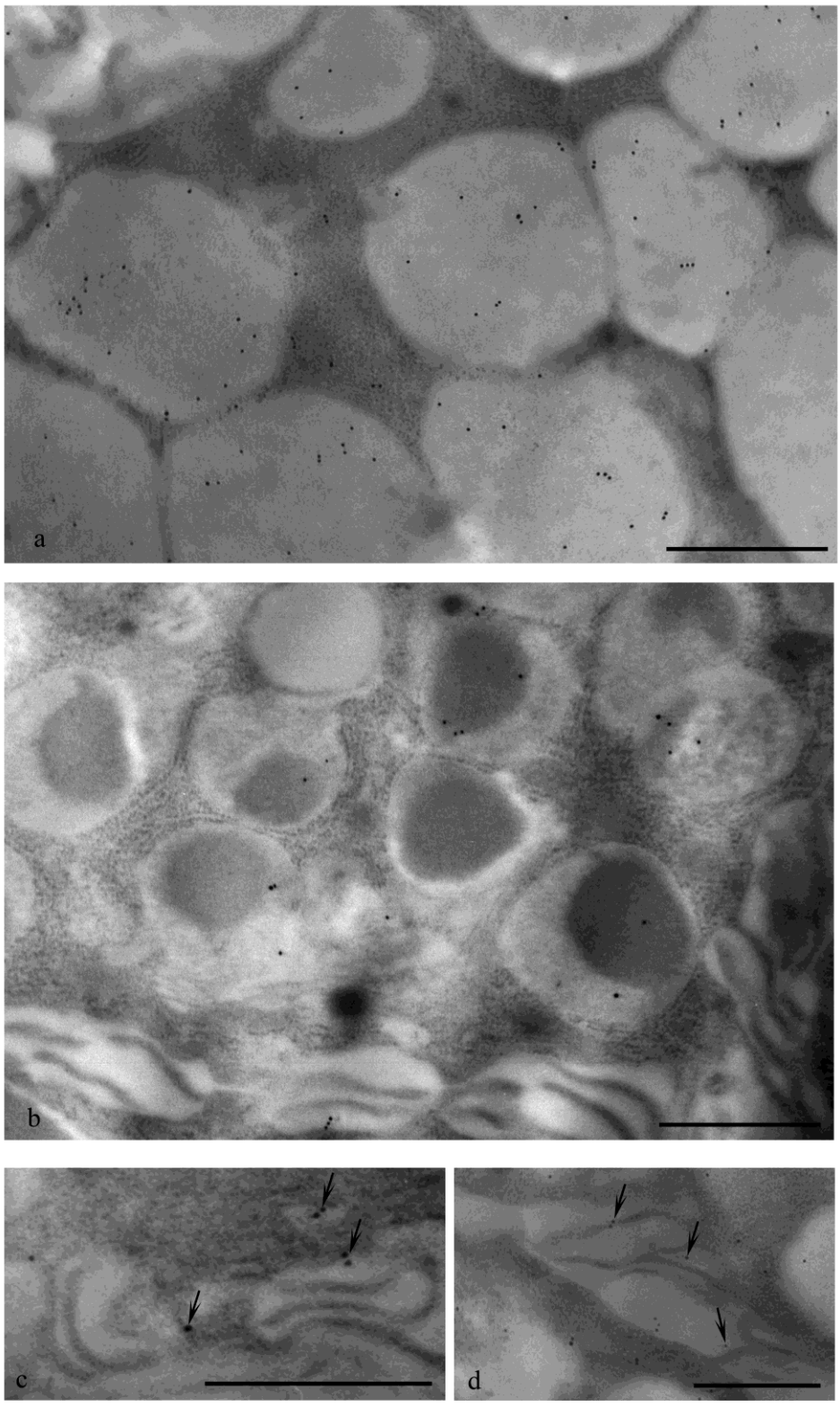


Fig. 10. TEM images of serous cells of parotid (a, c) and submandibular (b, d) glands stained for melatonin. In both glands, gold particles are preferentially associated with the secretory granules (a, b). The mere observation highlights a stronger reactivity in parotid with respect to submandibular gland. A moderate staining is observed also in basolateral membranes and small vesicles (c, d; arrows). Bar = 1 μm

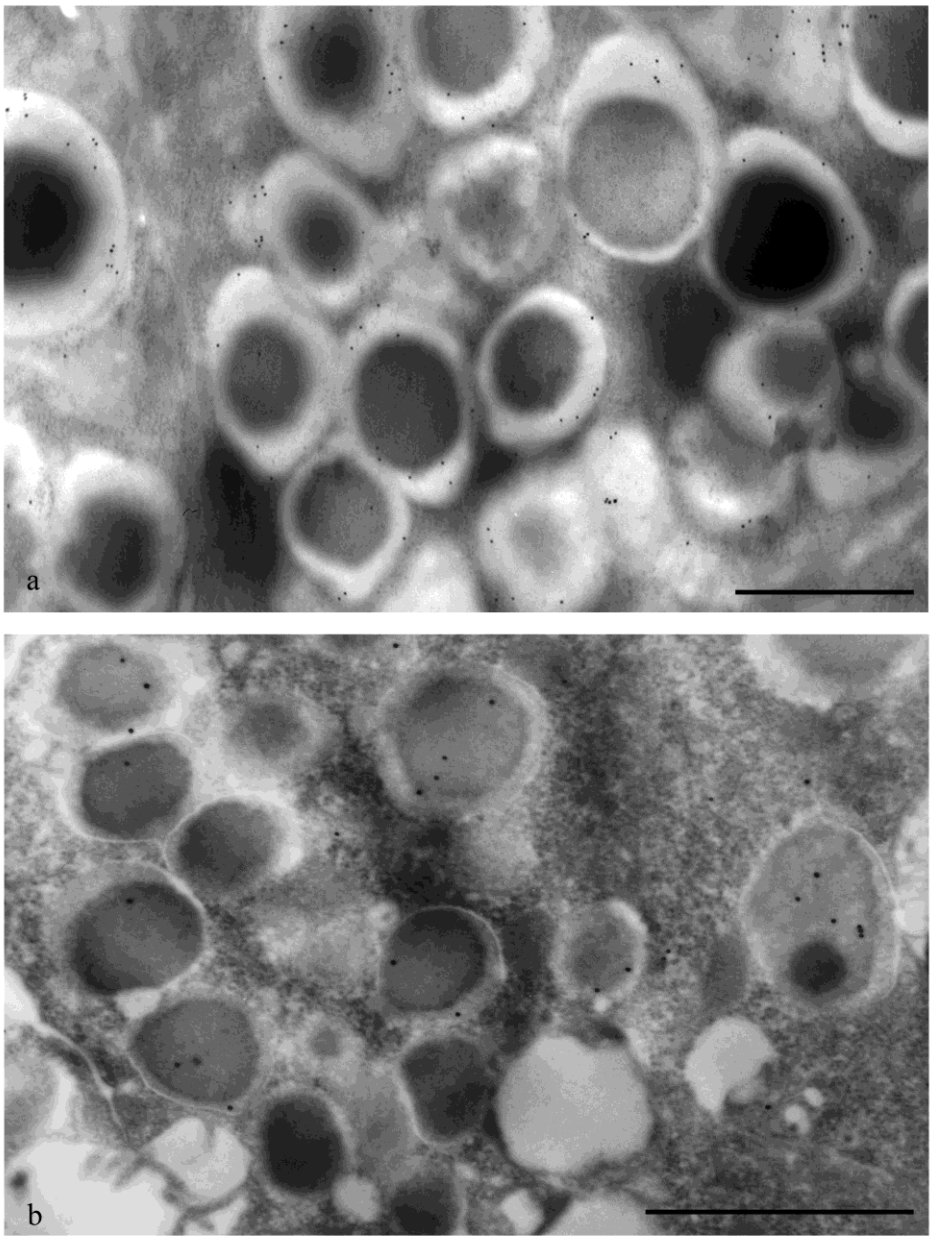


Fig. 11. TEM images of serous cells of diabetic parotid (a) and submandibular (b) glands stained for melatonin by immunogold. As in non-diabetic samples, gold particles specifically decorate secretory granules. Bar = 1 μm

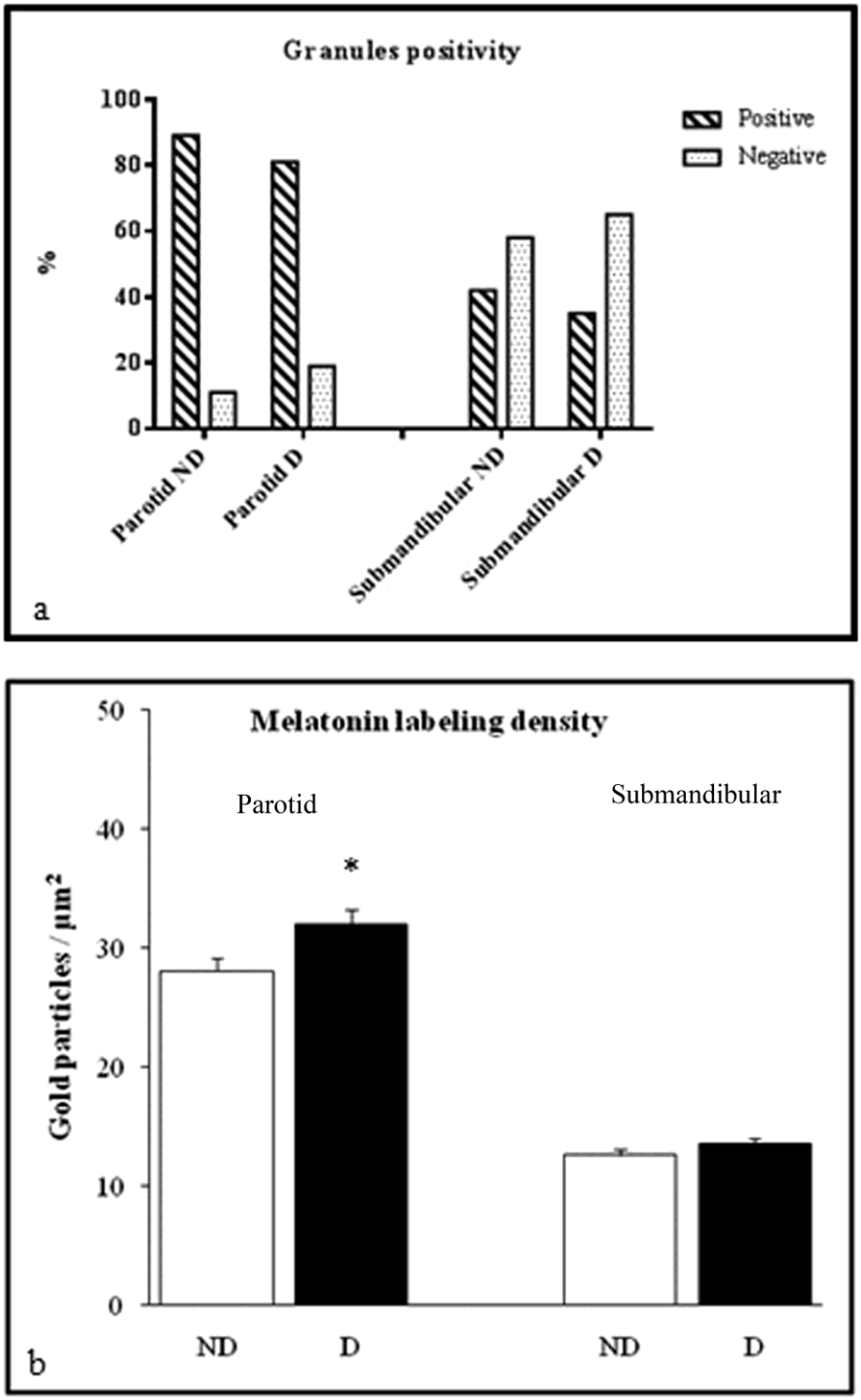


Fig. 12. Morphometrical evaluation of melatonin labeling density in serous granules. The percentage of labeled granules (a) decreases in diabetic glands (D). Melatonin labeling density (b) shows a significant diabetes-related increase (14%) in parotid glands, and a tendency to increase (7,5%) in submandibular glands. * $P < 0,05$

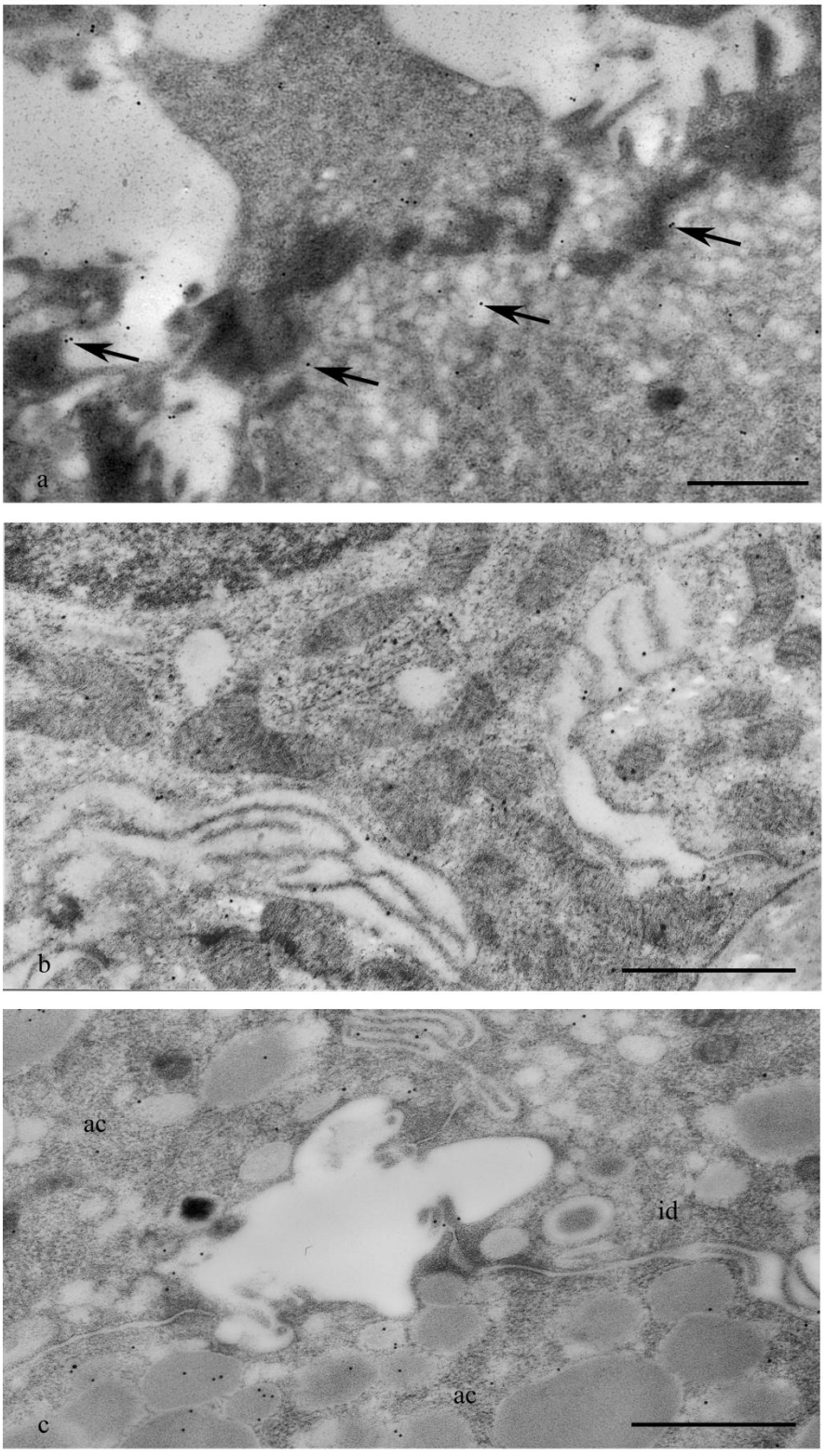


Fig. 13. TEM images of ductal cells of non-diabetic submandibular gland stained for melatonin. Striated ducts (a, b): apical (a) and basal (b) portions show a modest labeling within small vesicles throughout the cytoplasm and near the basolateral surfaces. Intercalated ducts (c): in intercalated duct cells (id) melatonin reactivity is only occasional. ac: acinar cells. Melatonin reactivity is identical in parotid, and does not change in diabetic glands (not shown). Bar = 1 μm

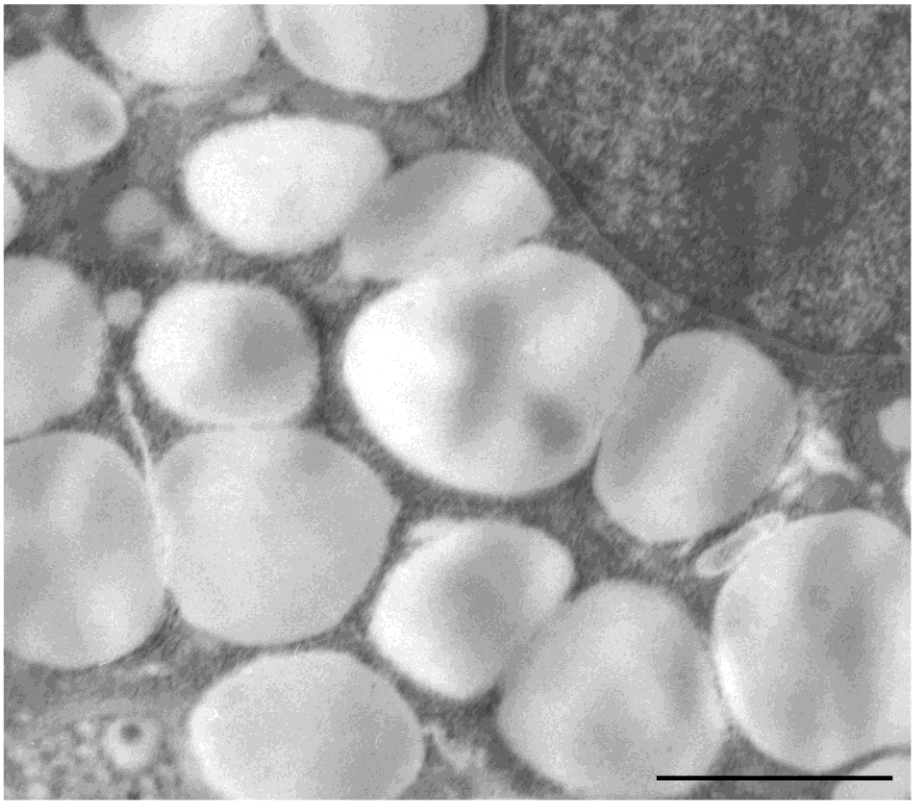

Fig. 14. TEM image of a portion of parotid serous cell used as a control. In all control experiments the melatonin staining is completely absent. Bar = 1 μm

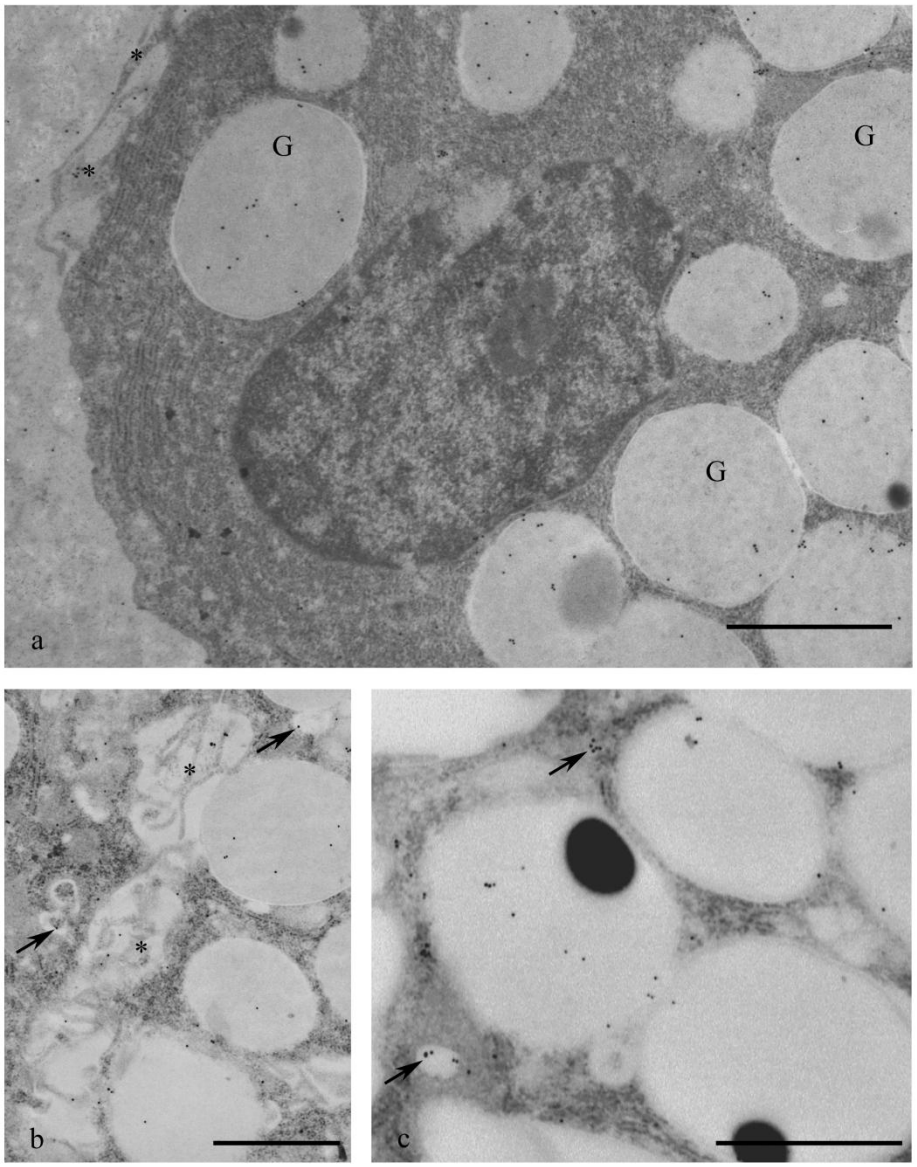


Fig. 15. TEM images of parotid acinar cells stained for MT1 receptor. a: gold particles are associated with secretory granules (G), and basal membranes (asterisks). b: lateral membranes (asterisks) are also reactive, as well as small vesicles (arrows). c: labeled vesicles (arrows) often appear among the secretory granules. Bar = 1 μm

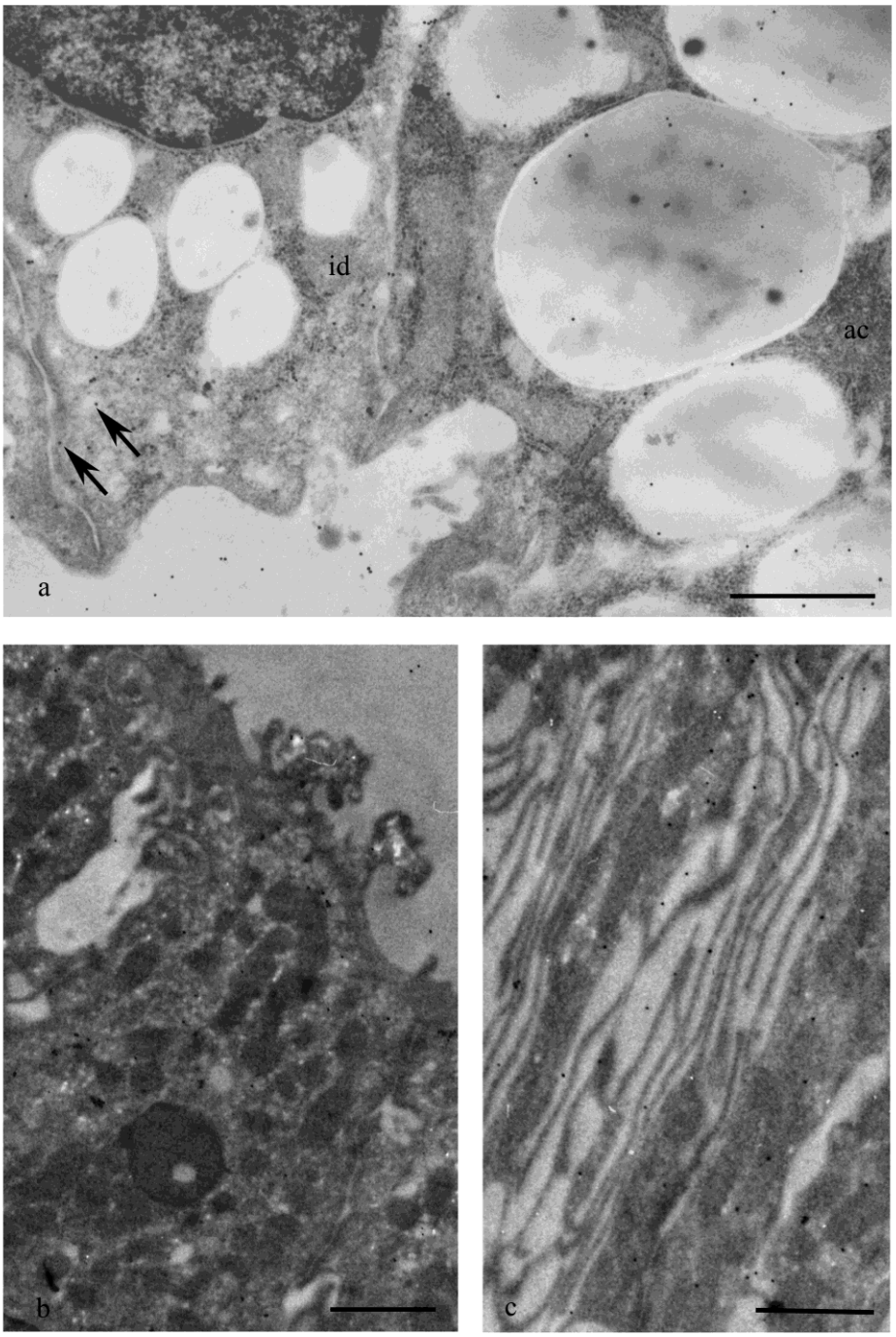


Fig. 16. Immunogold staining for MT1 receptor in parotid gland ducts. An intercalated duct cell (id) adjacent to an acinar cell is showed in a: vesicles near the luminal membrane are stained (arrows). Striated duct cells (b, c): a few labeled vesicles are seen in the cell apex (b), while a marked labeling is observed in basolateral membrane folds and vesicles (c). Bar = 1 μm

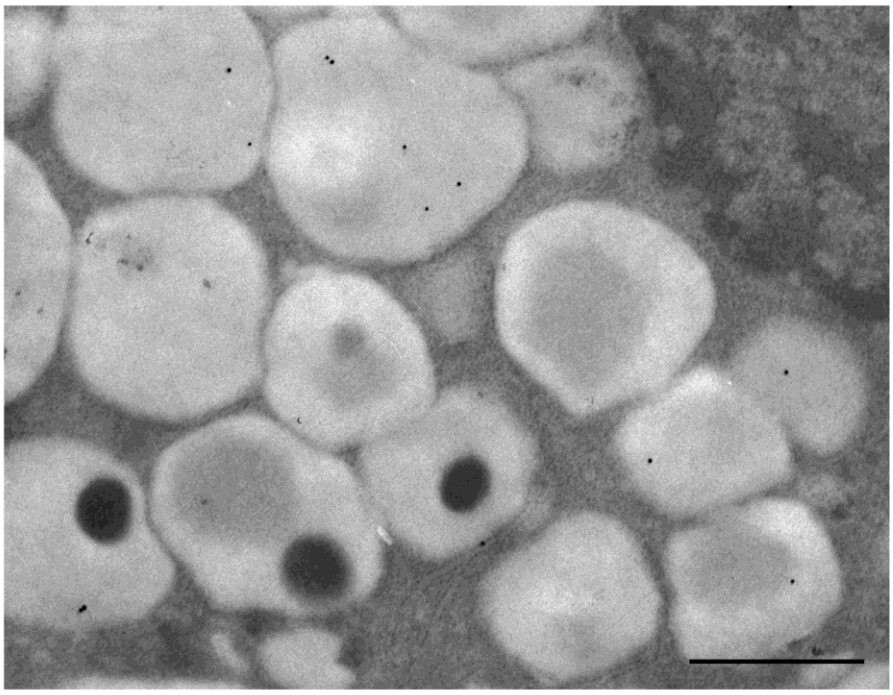

Fig. 17. Immunogold staining for MT2 receptor in parotid gland. The distribution pattern is the same observed for MT1, but the number of gold particles appears much smaller. Bar = 1 μm

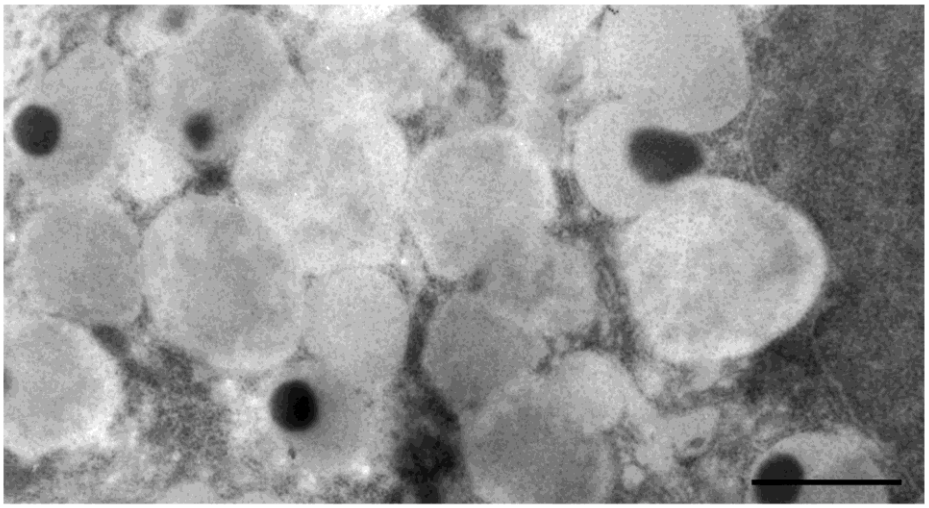

Fig. 18. TEM image of a parotid acinar cell representative of controls. MT1 and MT2 staining is completely absent. Bar = 1 μm

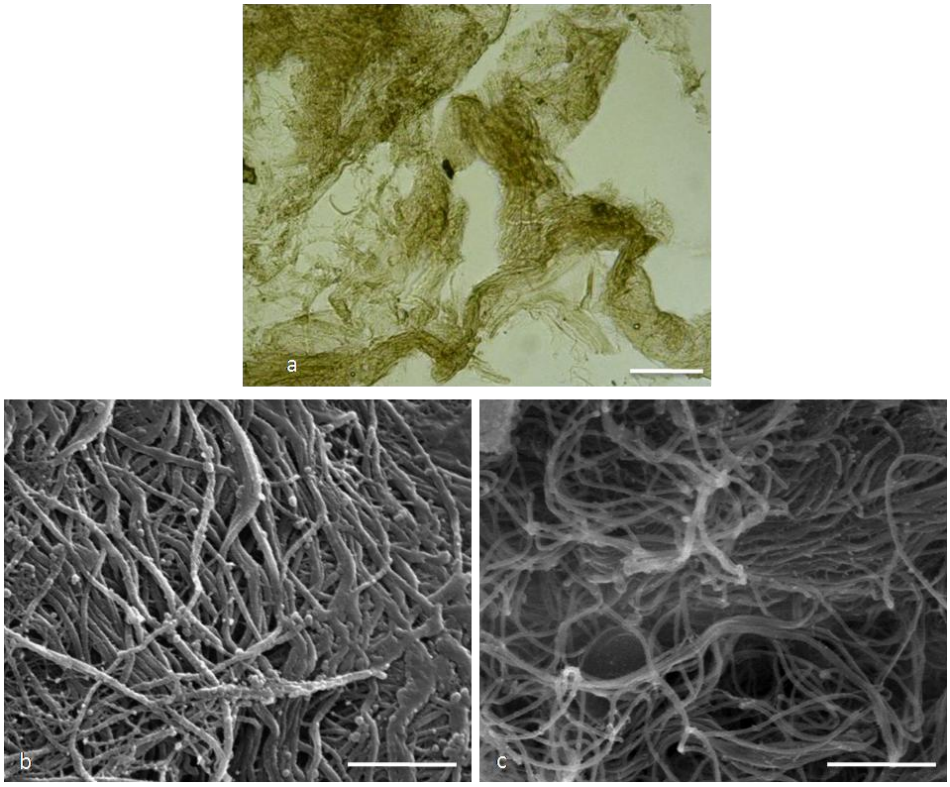


Fig. 19. a: Phase contrast microscope image of nHSMGS. Bar= 100 µm. b, c: HRSEM images of fibers in nHSMGS (b) and in the stroma of a human submandibular gland (c). Bar = 1 µm

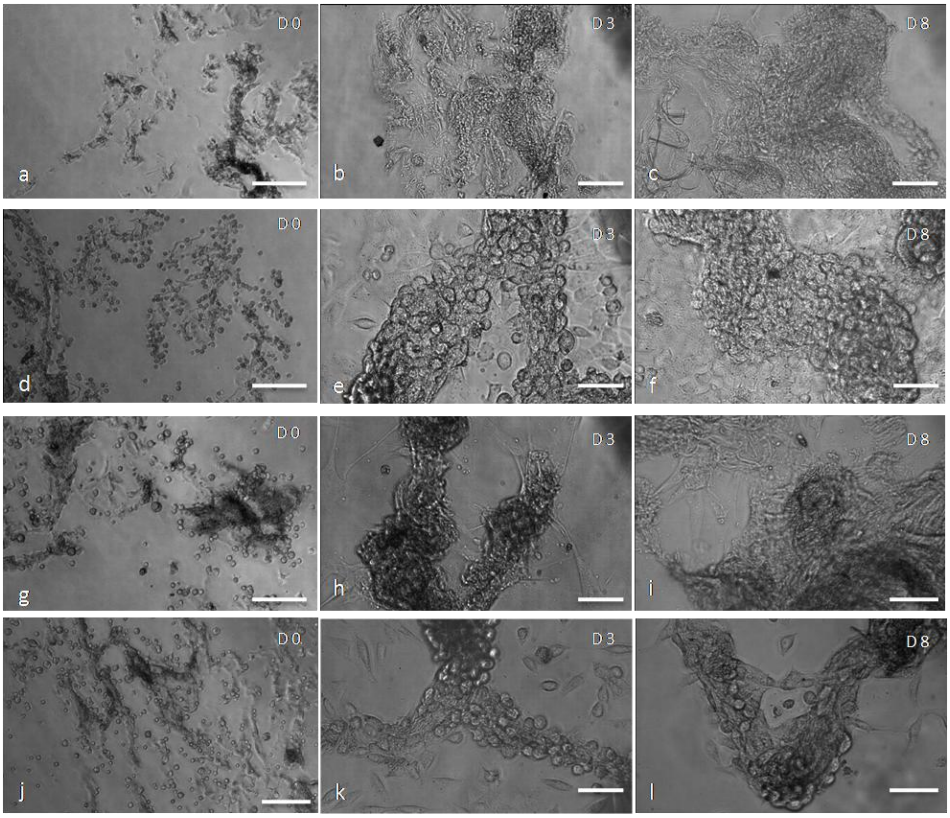


Fig. 20. Phase contrast images of nHSMGS (a, b, c) and nHSMGS + HSG (d, e, f), +HFF (g, h, i) and +HSG+HFF (j, k, l) at day 0 (D0), 3 (D3), and 8 (D8) of culture. HSG and HSG+HFF on nHSMGS always appears at higher cell density than HFF cells plated alone. D0 images Bar = 200µm; D3 and D8 images Bar = 70µm

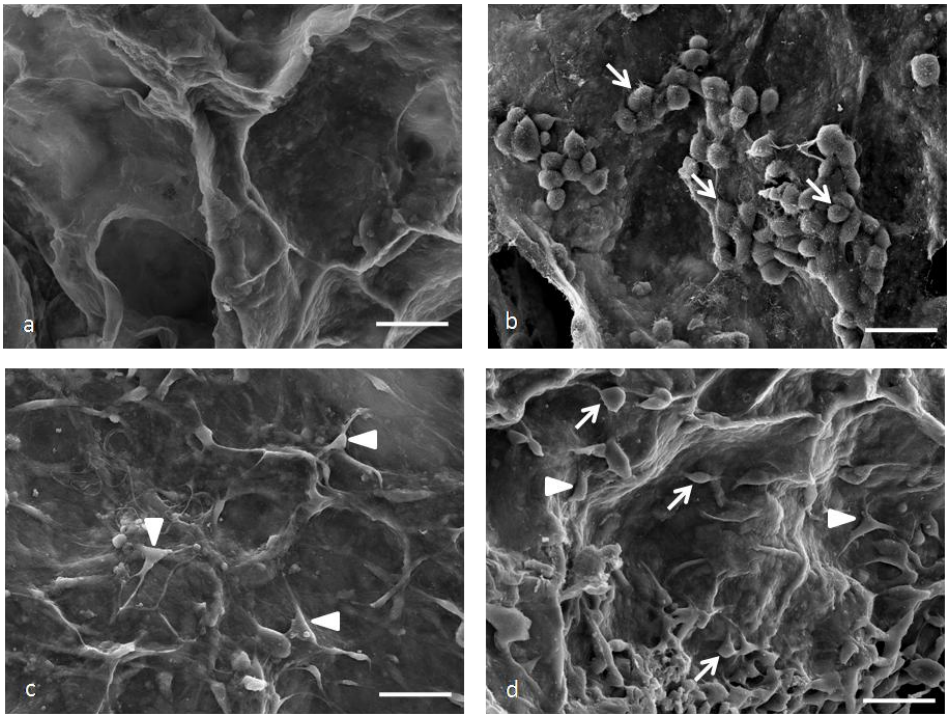


Fig. 21. HRSEM micrographs of nHSMGS without cells (a), nHSMGS + HSG (b), +HFF (c), +HSG+HFF (d). Low magnification images display the scaffold as an uniform surface (a) on which the cells lie (b, c, d). HSG (arrow) and HFF (arrowhead) are easily observable on top of the scaffold. Bar = 50μm

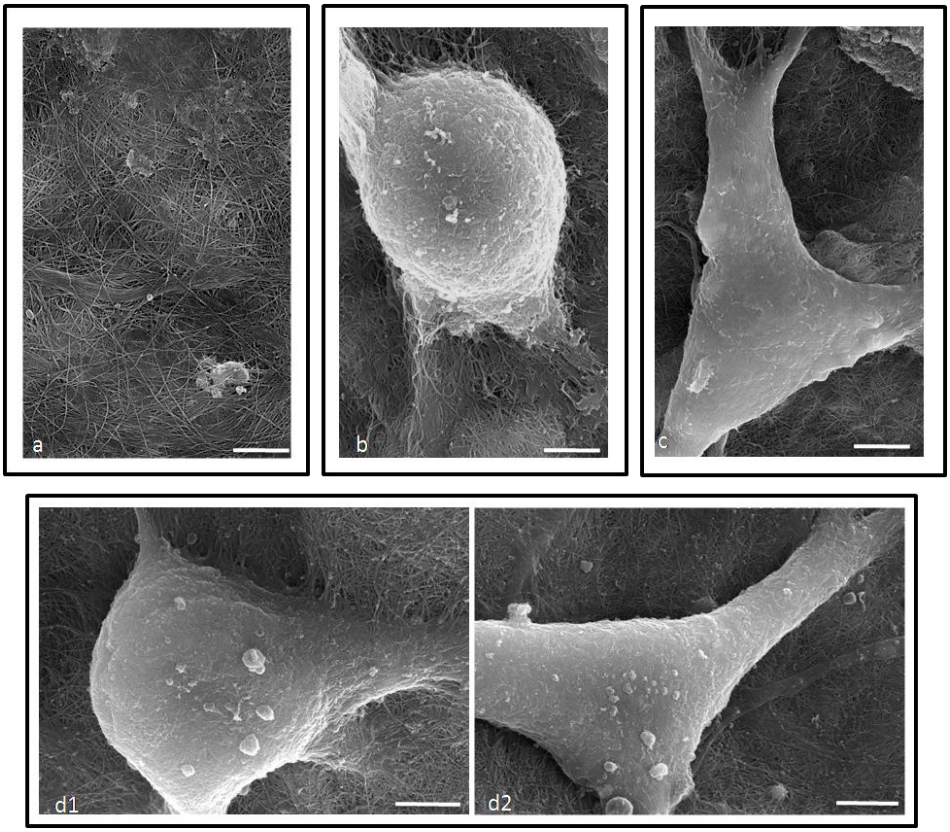


Fig. 22. High magnification of nHSMGS without cells (a), nHSMGS + HSG (b), +HFF (c), +HSG+HFF (d1,d2) by HRSEM. The processes by which cells anchored to the scaffold are visible in pictures b, c, and d. Bar = 3 μm

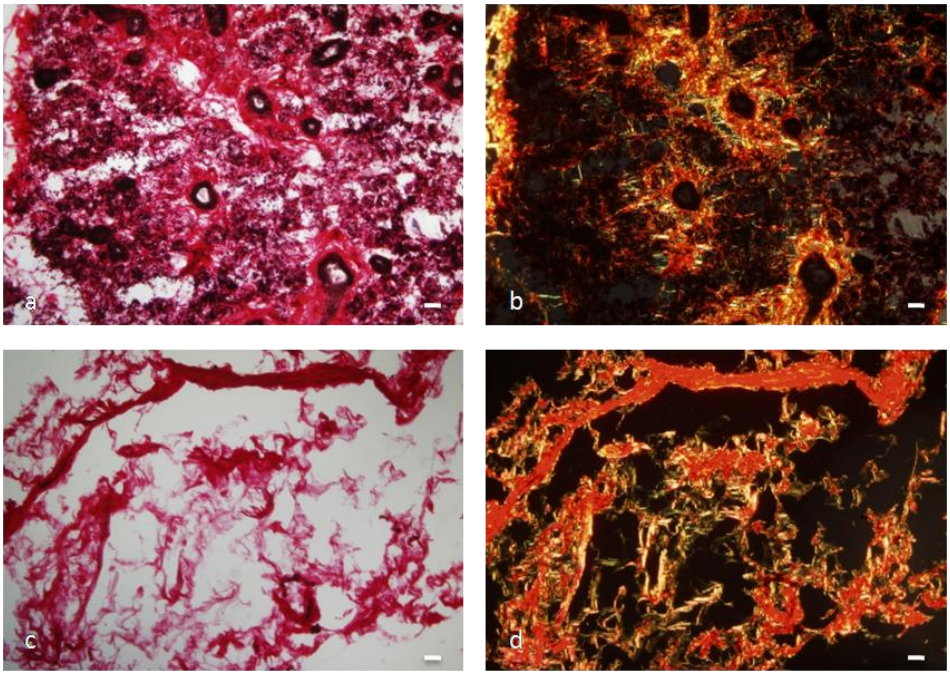


Fig. 23. Light microscope images of picro-sirius red staining in human submandibular gland (a, b) and in the nHSMGS (c, d). Samples photographed under bright–field light microscope are showed in figure a and c. In the submandibular gland (a) it is possible to recognize the acinar and ductal components. A network of fibers is observable in picture c. The same slides were observed under polarized microscope in order to detect collagen fibers (b, d). Collagen type I is represented by the thick yellow-red fibers, while collagen type III is visualized as a thin green fibers. Bar = 200 μm

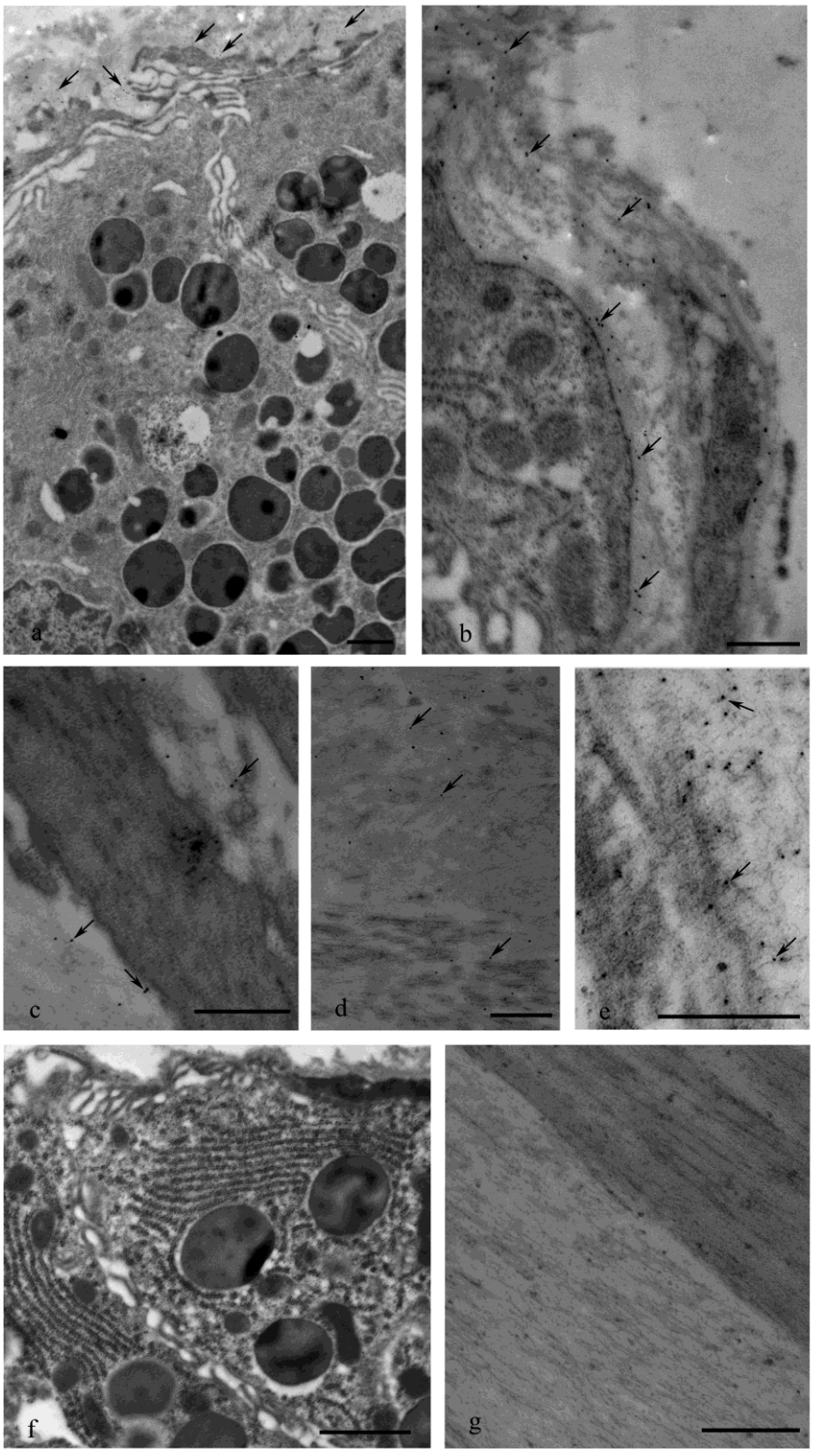


Fig. 24. Transmission electron microscope images of immunogold staining for collagen type IV. a, b: human submandibular gland; c, d, e: nHSMGS. Gold particles labeling the collagen type IV (arrows) are localized in the basal lamina of the intact gland (b), while in the nHSMGS in the amorphous masses and only occasionally in the electron dense fibers. In controls (f, g) no gold particle are observed. Bar = 1 μm

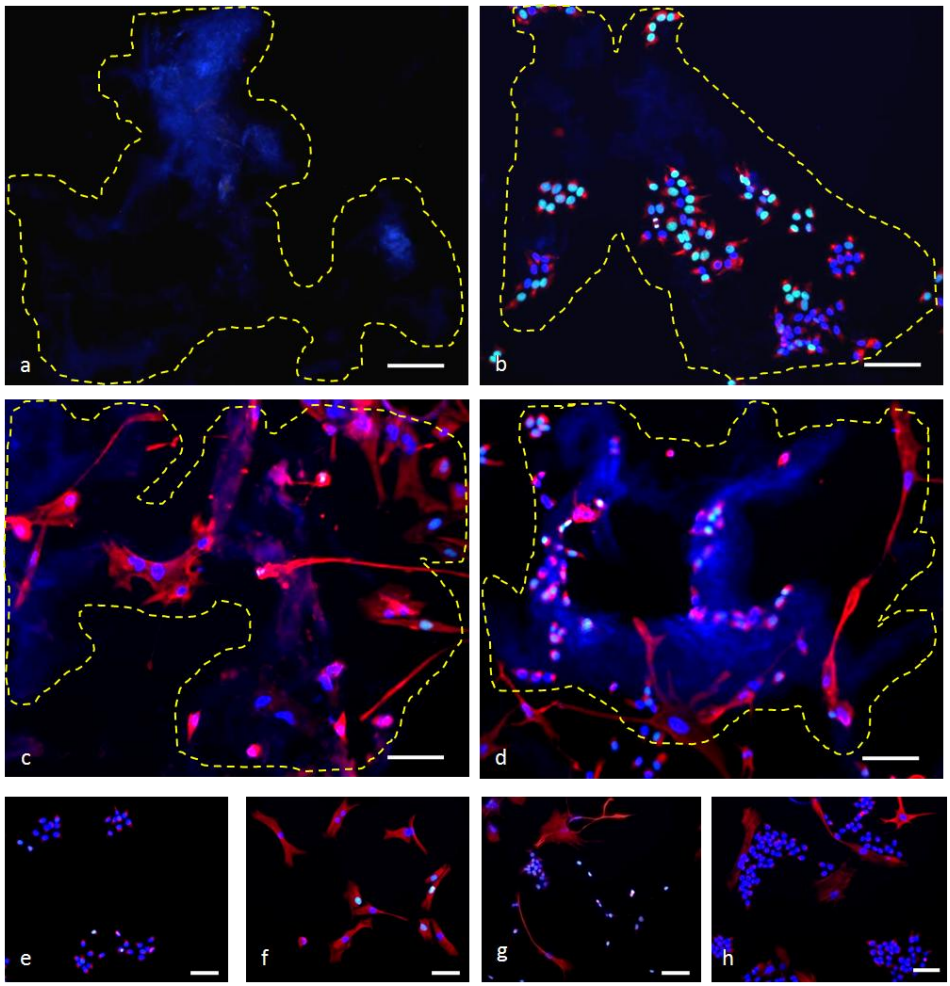


Fig. 25. Cell proliferation (click-Edu assay) in nHSMGS without cells (a), nHSMGS + HSG (b), +HFF (c), +HSG+HFF (d). Pictures e, f, g are respectively HSG, HFF and HSG+HFF cultured on glass, while HSG+HFF used as a control for the Edu assay (Edu was obmitted) are showed in h. Green: nuclei of proliferating cells; blue: nuclei of cells stained with Hoechst; red: cell cytoplasm stained with the rabbit anti-vimentin antibody. The nHSMGS outlined with yellow dashed lines is observable under microscope by the blue channel due to is natural fluorescence. Bar = 100 µm

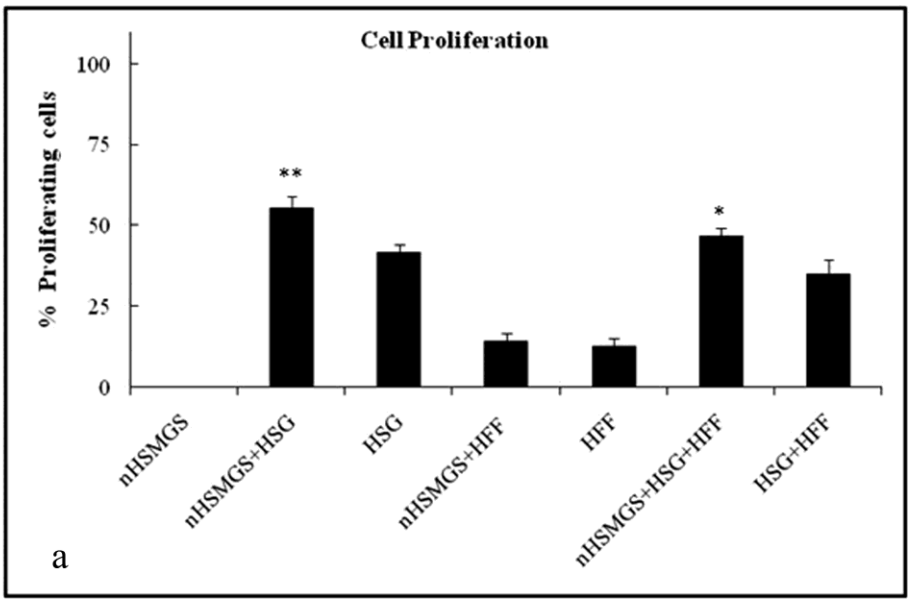


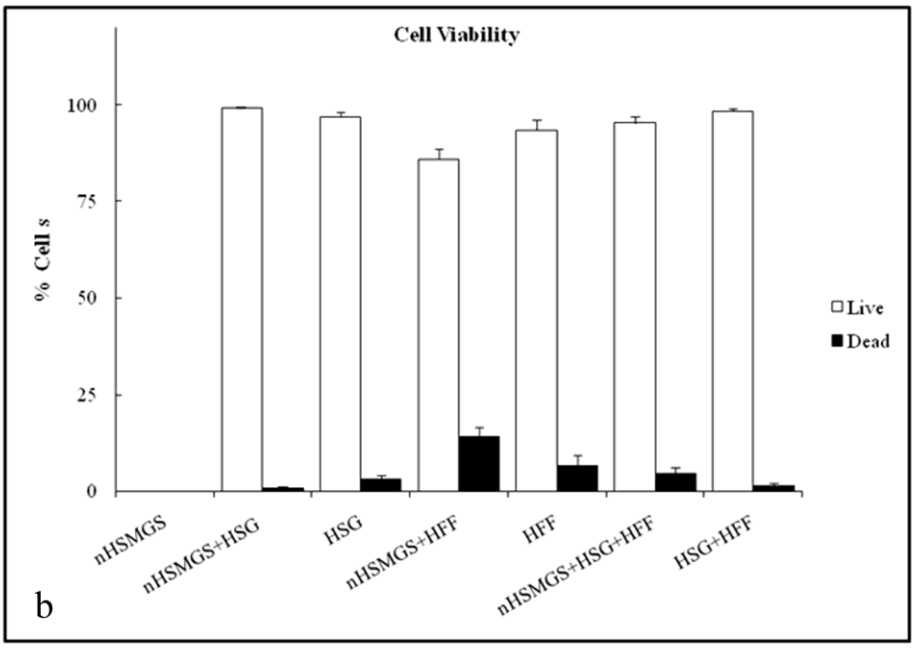


Fig. 26. a: Results of cell proliferation assay at day 4 of culture. HSG and the mixture HSG+HFF when cultured on the scaffold (nHSMGS+HSG and nHSMGS+HSG+HFF) exhibit an higher number of proliferating cells if compared to those cultured on glass (HSH or HSG+HFF). No differences are observed between fibroblasts cultured on scaffold (nHSMGS+HFF) and those cultured on glass (HFF). * $P < 0,05$; ** $P < 0,01$ . b: Results of cell viability assay after 8 days of culture. All cell types show a high level of live cells (white columns) either when cultured on scaffold or glass. No statistical significant differences were observed between the groups.

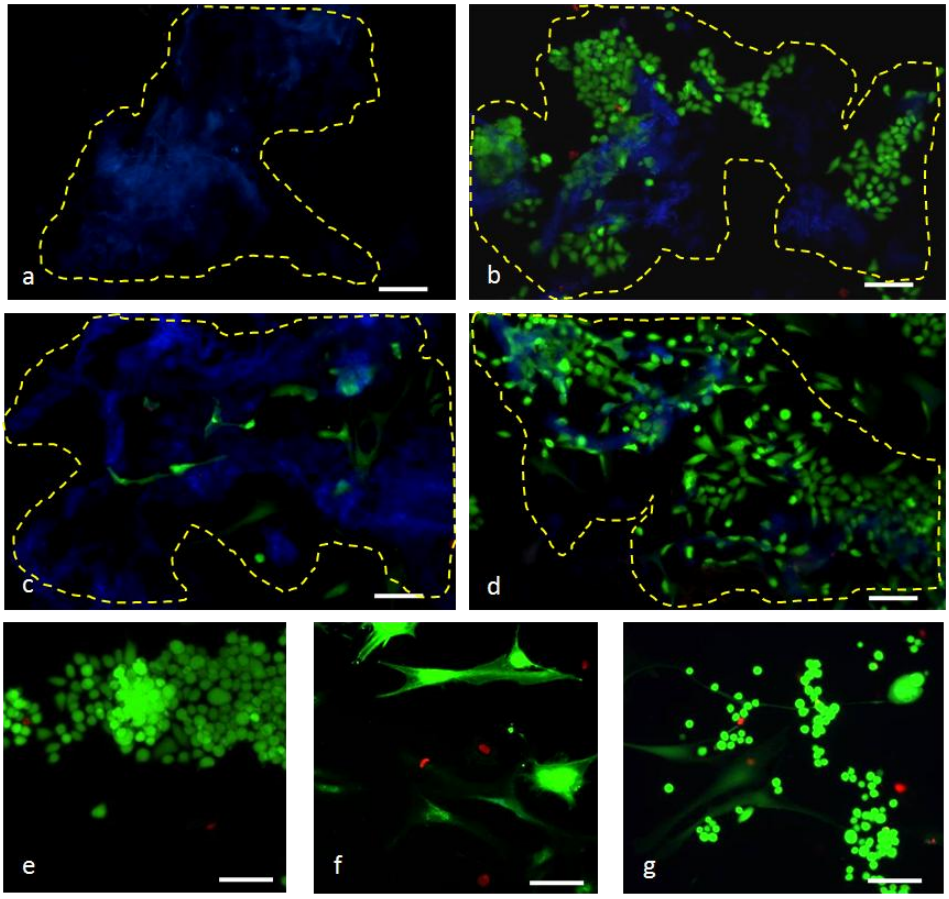


Fig. 27. Cell viability (Live/Dead staining) nHSMGS without cells (a), nHSMGS + HSG (b), +HFF (c), +HSG+HFF (d). Live cells stained with Calcein-AM show a green cytoplasm, while dead cells stained with Ethidium homodimer-1 show red nuclei. The nHSMGS outlined with yellow dashed lines is observable under microscope by the blue channel due to is natural fluorescence. Bar = 100 µm

## ACKNOWLEDGEMENTS

*I owe my deepest gratitude to my tutor Professor Margherita Cossu for introducing me into the research field of salivary glands and electron microscopy, and for her expert guidance, support and encouragement during my PhD experience.*

*I am deeply grateful to Professor Alessandro Riva, for his precious advices and for encouraging my research.*

*I express my sincere thankfulness to my co-tutor Dr Michela Isola, for her support, teachings, and supervision throughout these years, and to my colleagues Dr Raffaella Isola, Dr Francesco Loy, Dr Paola Solinas, Dr Alberto Casti, Dr Gabriele Conti, and Dr Martina Diana for their good advices, collaborations, and friendship. I would also like to thank Professor Jörgen Ekström for his valuable advices.*

*I have had the valuable opportunity to spend part of my PhD at the Faculty of Dentistry at McGill University, for that I would like to express my heartfelt gratitude to Professor Simon D Tran, for giving me the opportunity to work in his research group. I would also like to thank all the team members of the Laboratory of Craniofacial Tissue Engineering and Stem Cells, in particular Dr You-Joung Nicole Seo, Dr Ghada Abu-Elghanam, Dr Dongdong Fang, Dr Younan Liu, Dr André Charbonneau, Dr Mohamed Nur Abdallah, and Dr Shahul Hameed for their critical comments, suggestions, help, and friendship.*

*Lastly, I would like to thank my family and my friends for all their love and support.*

## LIST OF PUBLICATIONS

- **MA Lilliu**, F Loy, M Cossu, P Solinas, R Isola, M Isola. ***Type-2 diabetes affects the secretory activity of Human Parotid and Submandibular glands.*** (Submitted)

- **Lilliu MA**, Solinas P, Cossu M, Puxeddu R, Loy F, Isola R, Quartu M, Melis T, Isola M. ***Diabetes causes morphological changes in human submandibular gland: a morphometric study.*** J Oral Pathol Med. 2015 Apr;44(4):291-295.

- Solinas P, Isola M, **Lilliu MA**, Conti G, Civolani A, Demelia L, Loy F, Isola R. ***Animal models are reliably mimicking human diseases? A morphological study that compares animal with human NAFLD.*** Microsc Res Tech. 2014 Oct;77(10):790-796.

- Loy F, Isola M, Isola R, **Lilliu MA**, Solinas P, Conti G, Godoy T, Riva A, Ekström J. The antipsychotic amisulpride: ultrastructural evidence of its secretory activity in salivary glands. Oral Dis. 2014 Nov;20(8):796-802.

- Isola M, Ekström J, Diana M, Solinas P, Cossu M, **Lilliu MA**, Loy F, Isola R. ***Subcellular distribution of melatonin receptors in human parotid glands.*** J Anat. 2013 Nov;223(5):519-524.

- Setzu M, Biolchini M, **Lilliu A**, Manca M, Muroni P, Poddighe S, Bass C, Angioy AM, Nichols R. ***Neuropeptide F peptides act through unique signaling pathways to affect cardiac activity.*** Peptides. 2012 Feb;33(2):230-239.

## CONGRESS COMUNICATIONS

- Seo YJ, **Lilliu MA**, Lee JC, Zeitouni A, El-Hakim M, Tran SD. ***The Three-Dimensional Human Salivary Organoid Culture System Supports the Expansion of Functionally Secreting Acinar Cells in vitro.*** 10th Annual Reasearch day, Faculty of Dentistry, McGill University. Montreal, April 2nd 2015

- M Isola, F Loy, P Solinas, **MA Lilliu**, J Ekström, R Isola. ***Subcellular distribution of melatonin receptors in rat parotid salivary glands: effect of melatonin intravenous infusion.*** Italian Journal of Anatomy and Embryology. Vol.119, n.1 (Supplement): 105, 2014

- P Solinas, M Isola, **MA Lilliu**, F Loy, R Vargiu, R Isola. ***Cardiac mitochondria alteration and peripheral vessel morphology in female diabetes.*** Italian Journal of Anatomy and Embryology. Vol.119, n.1 (Supplement): 105, 2014

- Riva A, Loy F, Isola R, Isola M, Solinas P, **Lilliu MA**, Diana M, Conti G, Ekström J. ***Effects of antipsychotic drugs on human submandibular glands in vitro. An HRSEM morphological and morphometrical study.*** XXIII International Symposium on Morphological Sciences (ISMS) 2013

- **MA Lilliu**, P Solinas, R Puxeddu, M Cossu and M Isola. ***A morphometric study of human submandibular gland in type 2 diabetic status.*** Italian Journal of Anatomy and Embryology. Vol.118, n.2 (Supplement): 115, 2013

- P Solinas, **A Lilliu**, M Cossu, A Civolani, L Demelia and R Isola. ***Animal models are reliably mimicking human diseases? A morphological study that compares animal and human NAFLD.*** Journal of Anatomy and Embryology. Vol.118, n.2 (Supplement): 174, 2013

- Riva A, Loy F, Solinas P, **Lilliu MA**, Conti G. ***The discovery of the valves of the veins and its relevance to the knowledge of the movement of heart and blood.*** XXIII International Symposium on Morphological Sciences (ISMS) 2013

- M Isola, P Solinas, R Isola, M Diana, **MA Lilliu** , F Loy, J Ekström, M Cossu. ***Subcellular distribution of melatonin receptors in Human parotid gland.*** 35th National Congress of the Italian Society of Histochemistry, Pula (Cagliari), 12- 14 June 2013

- M Isola, **MA Lilliu**, R Isola, P Solinas, G Conti, M Diana, M Cossu, F Loy. ***Junctional complex in serous cells of Human submandibular gland after treatment with segretagogue drugs. A morphological and morphometrical study.*** Nanomed workshop. Dalla Nanomedicina al Brain Imaging; Pula (Cagliari), 17- 19 April 2013

- P Solinas, M Isola, F Loy, G Conti, M Diana, **MA Lilliu**, A Riva, R Isola. ***Mitochondrial ultrastructure and metabolism in a rat model of NAFLD.*** Nanomed workshop. Dalla Nanomedicina al Brain Imaging; Pula (Cagliari), 17- 19 April 2013

- A Riva, G Conti and **MA Lilliu.** ***Luigi Castaldi (Pistoia 1890- Firenze 1945) and his outstanding contribution to the history of Florentine wax***

***modeling*.** Italian Journal of Anatomy and Embryology. Vol.117, n.2 (Supplement): 163, 2012